ENERGY AND EXERGY ANALYSIS OF RENEWABLE ENERGY UTILIZATION IN CEMENT PRODUCTION

A Thesis Submitted to
the Graduate School of Engineering and Sciences of
İzmir Institute of Technology
in Partial Fulfillment of the Requirements for the Degree of

MASTER OF SCIENCE

in Energy Engineering

by

Pelin ALACA

January 2025

İZMİR

We approve the thesis of **Pelin ALACA**

Examining Committee Members:

Assist. Prof. Dr. Başar ÇAĞLAR
Department of Energy Systems Engineering, İzmir Institute of Technology

Prof. Dr. Gülden Gökçen AKKURT
Department of Energy Systems Engineering, İzmir Institute of Technology

Assist. Prof. Dr. Emrah BIYIK
Department of Energy Systems Engineering, Yaşar University

24 January 2025

Assist. Prof. Dr. Başar ÇAĞLAR
Supervisor, Department of Energy Systems Engineering, İzmir Institute of Technology

Prof. Dr. Mousa MOHAMMADPOURFARD
Co-Supervisor, Department of Energy Systems Engineering, İzmir Institute of Technology

Prof. Dr. Gülden Gökçen AKKURT
Head of the Department of Energy Systems Engineering

Prof Dr. Mehtap EANES
Dean of Graduate School of Engineering and Sciences

ACKNOWLEDMENTS

I would like to sincerely thank the individuals whose support, guidance, and encouragement were crucial to the successful completion of my master's thesis. Their contributions have been truly invaluable.

First of all, I would like to express my sincere gratitude to my advisor, Assist. Prof. Dr. Başar Çağlar, for his technical and motivational guidance throughout my master's thesis. I would also thank my co-advisor, Prof. Dr. Mousa Mohammadpourfard for his extensive knowledge and guidance.

I am grateful to my mother Havva, my father Musa, and my brother Cemal, for their support and encouragement. I am also grateful to my little bird Behlül for cheering me up during this period.

I have special thanks to Caglar Research Group and my colleagues for their encouragement and support during my thesis. I also have special thanks and gratitude to my partner Ata Barış for his infinite support and for always being by my side.

ABSTRACT

ENERGY AND EXERGY ANALYSIS OF RENEWABLE ENERGY UTILIZATION IN CEMENT PRODUCTION

The energy and exergy analysis of cement production was investigated to explore greener energy system alternatives in contrast to traditional cement production methods. Two different greener energy systems scenarios were considered. The base scenario was conventional cement production. In the first scenario, the pyrolysis of waste wind turbine blades and the gas turbine were integrated with the cement factory, where electricity demand was met by the gas turbine. At the same time, the raw material was provided from the solid residue of the pyrolysis unit. For this scenario a preheating system was considered to harness hot streams. In the second scenario, PEM electrolyzer was also included in the cement factory. In here hydrogen was produced from PEM electrolyzer to be replaced with coal. The thermodynamic modeling of all scenarios was conducted via Engineering Equation Solver (EES) software. The energy and exergy efficiency of the base scenario were found to be 61.60% and 20.21%, respectively. Other than thermodynamic analysis, specific energy consumption (SEC) and CO_2 emissions were calculated. The lowest SEC was obtained with scenario 1 which was 1704 kJ/kg. CO_2 emissions resulted minimum for scenario 2 with 0.219 kg CO_2/kg cement. Considering all of this, an attempt has been made to find a greener and less energy-consuming system.

ÖZET

ÇİMENTO ÜRETİMİNDE YENİLENEBİLİR ENERJİ KULLANIMININ ENERJİ VE EKSERJİ ANALİZİ

Geleneksel çimento üretim yöntemlerine kıyasla daha yeşil enerji sistemleri alternatiflerini keşfetmek için çimento üretiminin enerji ve ekserji analizi çalışılmıştır. İki farklı yeşil enerji senaryosu dikkate alınmıştır. Temel senaryo geleneksel çimento üretimidir. İlk senaryoda atık rüzgar türbini kanatlarının pirolizi ve gaz türbini çimento fabrikasına entegre edilmiştir ve elektrik ihtiyacı gaz türbini tarafından karşılanmıştır. Aynı zamanda hammadde piroliz ünitesinin katı ürününden sağlanmıştır. Bu senaryo için sıcak akımları kullanmak üzere bir ön ısıtma sistemi düşünülmüştür. İkinci senaryoda, PEM elektrolizörü de çimento fabrikasına dahil edilmiştir. Burada kömürle değiştirilmek üzere PEM elektrolizöründen hidrojen üretilmiştir. Tüm senaryoların termodinamik modellemesi Engineering Equation Solver (EES) yazılımı aracılığıyla gerçekleştirilmiştir. Temel senaryonun enerji ve ekserji verimliliği sırasıyla % 61,60 ve % 20,21 olarak bulunmuştur. Termodinamik analiz dışında, özgül enerji tüketimi (SEC) ve CO_2 emisyonları hesaplanmıştır. En düşük SEC, 1704 kJ/kg olan senaryo 1 ile elde edilmiştir. CO_2 emisyonları, 0,219 kg CO_2/kg çimento ile senaryo 2 için minimum olarak sonuçlanmıştır. Tüm bunlar göz önüne alınarak, daha yeşil ve daha az enerji tüketen bir sistem oluşturulmaya çalışılmıştır.

TABLE OF CONTENTS

LIST OF TABLES

Table **Page**

LIST OF FIGURES

Figure **Page**

CHAPTER 1

INTRODUCTION

Wind turbines play an important role as the world moves towards renewable energy sources to meet its energy needs. Although this technology is known to be environmentally friendly, it has caused an unexpected environmental problem: wind turbine waste. In particular, the fact that the large and durable blades of wind turbines cannot be recycled causes this equipment to become a waste problem that fills up landfills at the end of their lifespan. These blades, produced from fiberglass and composite materials, exhibit structures that are difficult to process with current recycling methods, and this creates significant challenges both economically and environmentally. In this context, the need to address the environmental impacts of sustainable energy solutions holistically emerges.

Liu and Barlow (2017) focused on the manufacturing and end-of-life (EOL) stages of waste wind turbine blades and stated that the annual amount of waste started to increase with the installation of new turbines starting from 2018. It is predicted that this waste will exceed 2 million tons (Mt) of blade waste per year by 2050 as it can be seen in Figure 1. It is also stated that 40% of this waste will be found in China, 25% in Europe, 16% in the USA and 19% in the rest of the world.

There are many different methods to dispose of the waste wind turbine blades. These methods can be considered from distinct perspectives. Each has its strengths and weaknesses. For instance, landfill and incineration seem like basic methods at first glance. However, landfills are banned because they cause environmental pollution. In addition, incineration is not a sustainable option due to the toxic substances it emits into the environment (Cheng et al. 2023; Kalkanis et al. 2019). Accordingly, cleaner approaches are needed to ensure sustainability.

In addition to these methods, mechanical, thermal and chemical methods are used to recycle waste blades (Jani et al. 2022). Pyrolysis is a thermochemical process and maintained in the absence of oxygen to thermally decompose the carbon-containing

materials at 300-1200 °C (Yang, Kim, and Lee 2022). About 90 wt% composite material is found in a standard wind turbine blade. This composite material is mostly a polymer composite reinforced with glass fiber and carbon fiber (P. Liu and Barlow 2016). In the pyrolysis process, polymer composites decompose, and then oil, gas, and char products are obtained. The solid char products are recovered as fibers, which is the desired output (Kalkanis et al. 2019). This is because pyrolysis is performed in the absence of oxygen, creating a mild process condition. So, recovered fibers remained nearly unchanged (Xu, Ji, Wu, et al. 2023). Furthermore, oil and gas products collected from pyrolysis could be reused to sustain energy in the system.

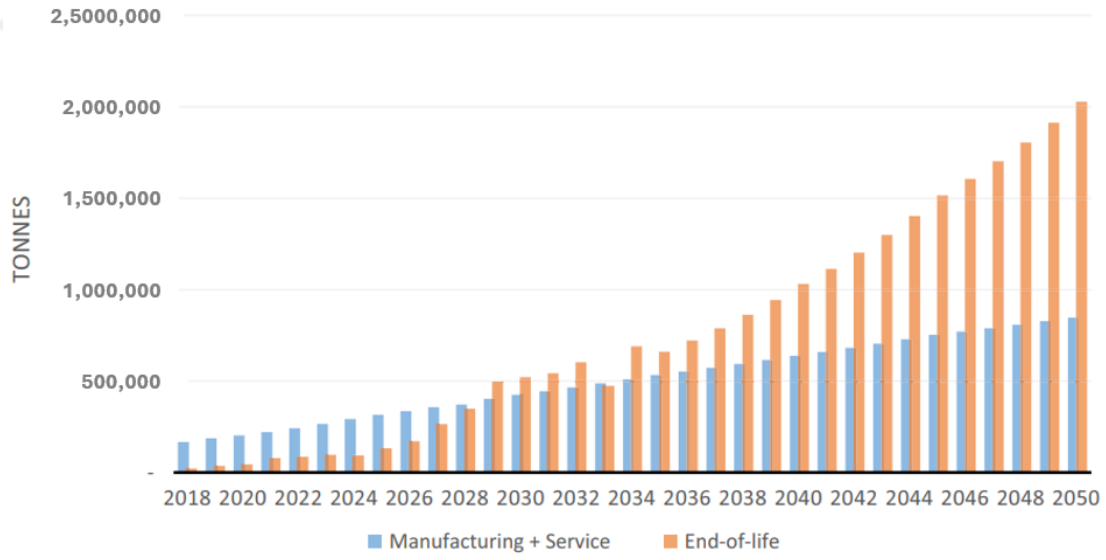

Figure 1. Global wind turbine blade waste estimation until 2050 (Source: Liu and Barlow 2017).

The similarity of chemical composition of wind turbine blade waste and the raw materials used in cement production offer a promising solution for the evaluation of these wastes in cement production. Wind turbine blades are generally produced from composite materials consisting of fiberglass and resins (Xu, Ji, Meng, et al. 2023). These materials are preferred due to their high strength and durability properties. The basic components of the blades include substances such as silica, calcium and aluminum oxide as shown in Table 1. These components are largely similar to the feedstock of cement production.

Raw materials required for cement production consist of limestone (calcium carbonate), clay (silica, aluminum oxide) and other additives raw material inputs from a cement facility are given in Table 2. During the production process, these raw materials are combusted at high temperatures to obtain an intermediate product called clinker. The compatibility of the oxides used in clinker production with the components found in turbine blades makes it possible to use wind turbine wastes in cement production.

The use of wind turbine waste in cement production can provide both economic and environmental benefits. Turbine blades contain composite materials with high energy density. These materials can be used as alternative fuels in cement kilns and reduce dependence on fossil fuels. The silica and calcium content in turbine blades can be used directly as additives in cement production. This contributes to sustainable production by reducing the consumption of natural resources.

Cement is a significant building material and has one of the highest production amounts in the world. The production amount of cement is assumed to be 4.1 billion tonnes in 2022 (Cembureau 2023). It is nearly produced in all countries because of the abundance of raw materials such as limestone. The main producers of cement are China, India, the EU, the US and Japan (Worrell 2014).

The production of cement is an extremely energy-intensive process. Its energy cost generally accounts for approximately 30-40% of the manufacturing cost (Madlool et al. 2012). It consumes about 5% of the world's total industrial energy. Globally, the cement industry is the third-largest industrial energy consuming sector and the second-largest industrial CO2-emitting sector (IEA 2018). The primary fuel of the cement process is coal, which is carbon-based and emits lots of CO_2 when burned. In addition to CO_2, NO_x, SO_x and particulate matter emissions could be observed during combustion (Worrell 2014). It is responsible for 6% percent of the world's GHG (greenhouse gas) emissions, and it is shown in Figure 2. The majority of emissions are due to the high amount of CO2 emissions generated during the calcination of limestone for clinker production (Marmier 2000). In the report of World Economic Forum 2024, several ways to reduce carbon emissions are pointed out. These are replacing $CaCO_3$ (limestone) with non-carbonate materials, replacing fuel with a decarbonized electricity source and using carbon capture technologies (WEF 2024).

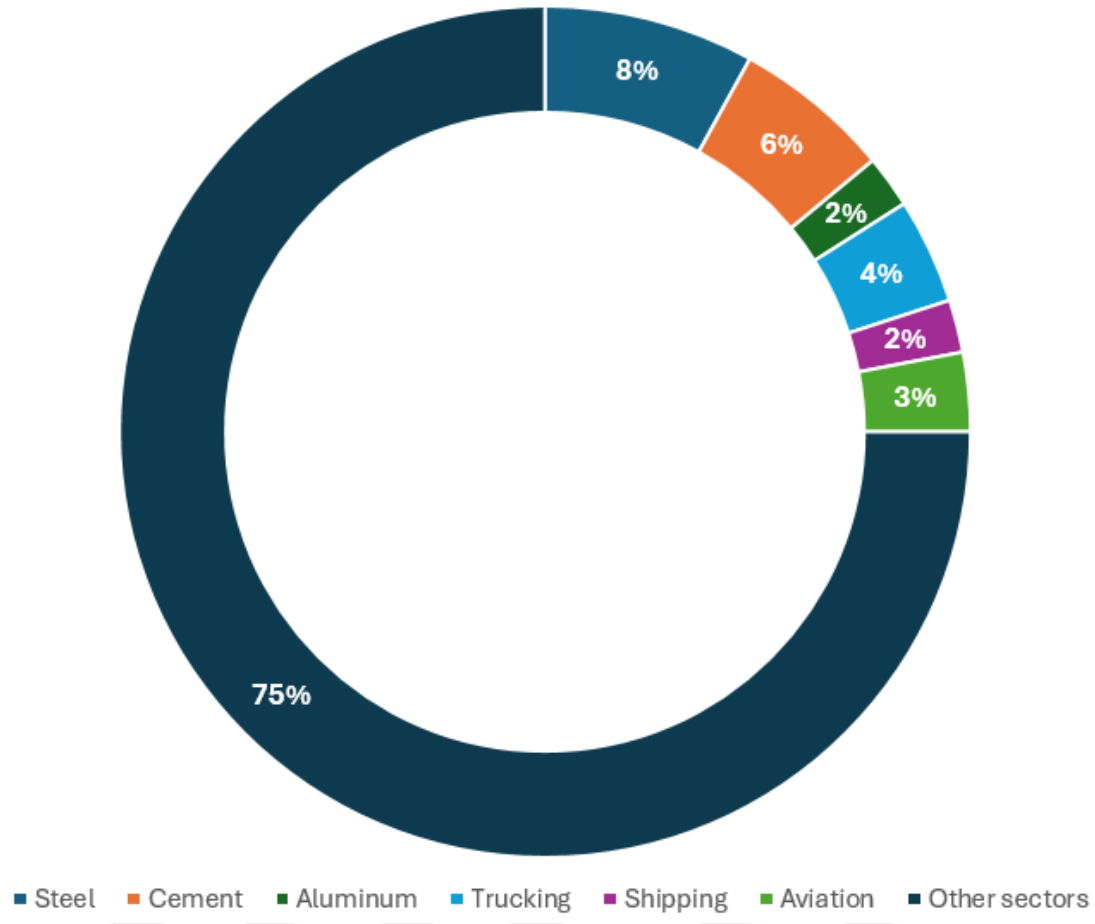

Figure 2. Global greenhouse gas (GHG) emissions, by sector (Source: WEF 2024).

Cement is mainly formed by limestone, clay and silica and used to produce concrete which is the world's most commonly used material (Atmaca 2014). The cement production process is an energy-intensive process that involves processing natural raw materials. Production usually begins with mixing limestone, clay, silica sand and iron ore in certain proportions. This mixture is heated in rotary kilns at approximately 1500°C to transform into an intermediate product called "clinker". During this high-temperature process, the calcium carbonate in the limestone decomposes into calcium oxide with the release of carbon dioxide (Singh and Shah 2023). The clinker is then cooled and ground into a fine powder. In the final stage, gypsum is usually added to the clinker to adjust the setting time of the cement. This fine powder obtained is packaged and shipped to be used for different purposes, such as concrete production in the construction sector (Atmaca 2014).

Six main processes exist to produce cement and they are as follows: crusher to crush the raw materials, blending the farine in raw mill, increasing the temperature of farine by precalcination in pyroprocessing tower, burning the farine in rotary kiln, grinding the clinker product in cement mill and finally packaging the final product (Atmaca 2014). These processes were represented in Figure 3.

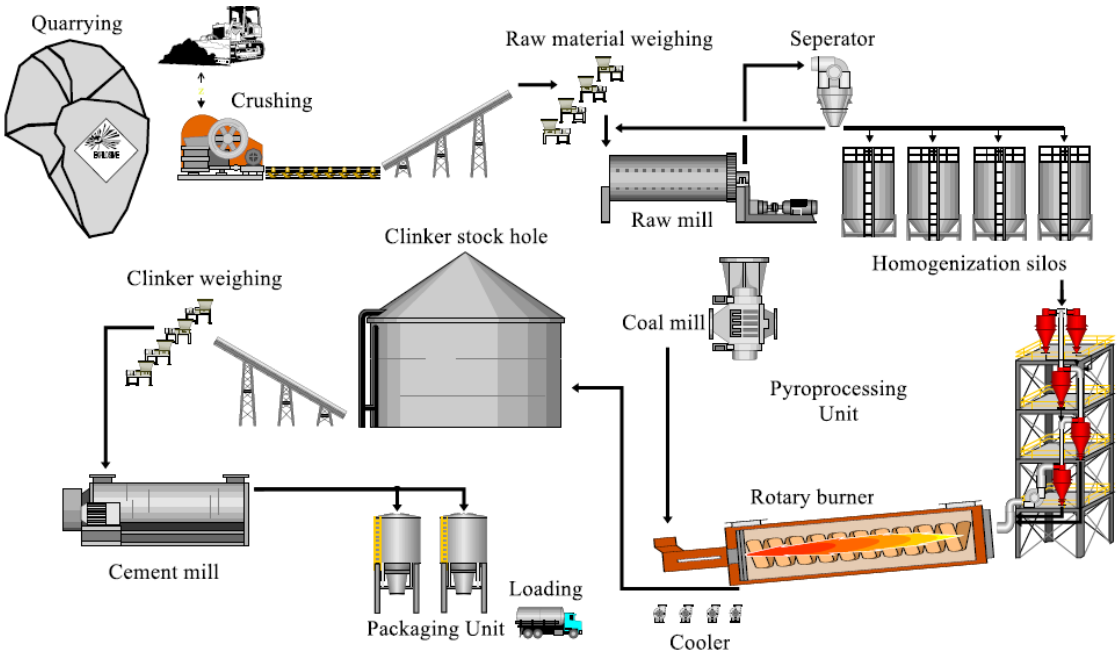

Figure 3. Cement production process scheme (Source: Atmaca 2014).

Basic chemical reactions in cement production involve calcination of limestone to produce calcium oxide, then reacting with minor substances that consists of SiO_2, Al_2O_3 etc. while evaporating all the moisture. Rotary kiln is the most energy consuming unit in the overall process since the temperature varies between 1300 ºC to 1600 ºC depending on the raw materials features. In addition, the calcination reaction takes place at 950 ºC. Main reactions take place in cement production are given as follows;

$$CaCO_3 \rightarrow CaO + CO_2 \quad (calcination\ reaction)$$

$$2CaO + SiO_2 \rightarrow Ca_2SiO_4\ (belite\ formation)$$

$$3CaO + SiO_2 \rightarrow Ca_3SiO_5\ (alite\ formation)$$

Wind turbine blades are usually made of composite materials such as fiberglass and resin, which can cause environmental problems by making them difficult to recycle. However, using these wastes as raw materials in cement production or subjecting them to the pyrolysis process to obtain fuel can propose a sustainable solution. Waste turbine blades containing fiberglass can contribute to the cement matrix because of its compatibility with cement production feedstock as stated above. In addition, obtaining liquid and gaseous fuels from turbine wastes through the pyrolysis process allows both energy recovery and waste disposal. Therefore, during the pyrolysis process, organic resins in turbine blades can be decomposed at high temperatures and used as fuel, while the remaining mineral content can be evaluated for use in cement production. Furthermore, cement units require electricity to function. This electricity can also be obtained through the gas turbine operated with fuels obtained from pyrolysis. By this way, dependency on grid electricity could be eliminated. This integrated approach both reduces environmental impacts and creates an economic advantage by saving energy and raw materials in the cement process.

Cement production is an energy intensive process as indicated above. A combined system integrating cement production, pyrolysis and gas turbine technologies offers significant opportunities in terms of both energy efficiency and sustainability. Energy and exergy analyses are critical to comprehend the system. Energy analysis determines the total amount of energy used in different components of the system and the energy flow, while exergy analysis evaluates energy quality, losses, and recovery potential.

In this study, energy and exergy analysis of a system containing pyrolysis of wind turbine blade wastes integrated into a cement facility were performed. Along with the pyrolysis and cement processes, a Brayton cycle and electrolyzer were included in the system to successfully generate electricity via gas turbine from the pyrolysis outputs (oil and gaseous products) to sustain energy to the cement facility and the overall process. Moreover, solid products obtained from the pyrolysis were used as raw material additives to feed into the cement process. Thermodynamic calculations were maintained by using Engineering Equation Solver software.

Energy and exergy analysis of cement production combined with the pyrolysis of waste wind turbine blades have been rarely addressed in the literature. This work was conducted to eliminate this deficiency. Most importantly, this study reveals the potential benefits and development areas of the combined system by performing energy and exergy

analysis. In this way, it is aimed to contribute to the literature and create a guide for future research and applications.

1.1. Aim and Content of the Thesis

The main objective of the thesis is to evaluate the performance of renewable energy alternatives to meet the energy load of the cement industry in a greener way. The specific objectives of the thesis are:

- To determine greener renewable energy alternatives to meet the heat and electricity demand of a cement factory.
- To develop thermodynamic models for the selected renewable energy systems integrated with a cement factory.
- To evaluate the performance of all considered systems by energy/ exergy analysis, SEC (specific energy consumption) and CO_2 emissions
- To determine the best scenario among the selected systems and to identify potential benefits and challenges for the implementation of the proposed systems.

To achieve the objectives, the thesis was structured as follows: In Chapter 2, a literature review was conducted on the cement industry, wind turbine blade wastes, pyrolysis, PEM electrolyzer, and energy and exergy efficiency of various renewable systems. In Chapter 3, the modeling of scenarios was explained in detail and processes described. In addition, definitions of energy and exergy analyses of these systems were given. In Chapter 4, results were presented and discussed. In Chapter 5, all the findings were gathered, and the best option was decided.

CHAPTER 2

LITERATURE SURVEY

Literature review on energy and/or exergy analysis of cement production, pyrolysis and electrolysis were described in this chapter.

Research about energy and exergy analysis of cement production was explained below. In the study of Koroneos, Roumbas, and Moussiopoulos (2005) cement production in Greece is analyzed using energy and exergy analysis and efficiencies are found as 68% and 50% respectively. A high amount of exergy loss is due to the combustion of pet coke, which is used as the primary fuel source in this study. Atmaca and Yumrutaş (2014) studied the thermal analysis (energy and exergy) of a cement plant located in Gaziantep, Turkiye. They investigated the most energy-intensive units in the process and tried to reduce fuel consumption to operate the system. In addition to the energy and exergy analysis, economic and environmental analyses were completed. As a result, an alternative fuel to coal is needed to reduce pollution. Better insulation is required to improve the plant performance (by decreasing exergy destruction) and reduce the cost (Atmaca and Yumrutaş 2014). The study of Ghalandari (2022) focuses on both decreasing greenhouse gas emissions and reducing the system's energy consumption. To achieve that goal, pyro-processing system was considered, where the clinker is produced. The effects of several parameters like feed rate and air temperature were examined. The energy and exergy efficiency of the pyro-processing system was calculated as 82.5% and 64%, respectively. Jalili et al. (2020) proposed a system that recovers heat from exhaust gas to the cement process. Thermodynamic analyses were completed using EES Software. The heat is recycled with thermodynamic cycles. In this way, both the gas emissions were reduced, and efficiency enhanced. Various cycles were proposed, and parametric studies were completed. The effect of turbine temperature and pressure on network output was studied. The exergy efficiency was improved when the inlet expanded the working fluid temperature, and the pressure of the turbine was near the critical points. In the study of Abutorabi and Kianpour (2022), recovery of wasted heat in cement plant is investigated. The purpose was to decrease fossil fuel use and GHG emissions. The boilers were placed

at the outlet of a clinker cooler and a preheater for heat recovery by using three different fluids (water, R134a and R245fa). The energy and exergy analysis results were obtained for a Rankine cycle and water use performed a higher exergy efficiency than the other fluids in the study. Additionally, R134a could be the most convenient fluid because it reduces 4.1% of the total exergy loss and shows an increment in the production capacity from 5 to 9 MW. Emyat (2020) points out that rotary kiln in the cement process leads to high amounts of energy and exergy losses during pre-calcining and pre-heating. By the heat lost during these processes, 300 kW of cooling effect could be obtained by recovering waste heat. That recovery process is called vapor absorption refrigeration system and decreasing fuel consumption and environmental impact are the other benefits of the system. Nami and Anvari-Moghaddam (2020) examined waste heat recovery by CCHP (combined cooling, heat and power) systems for a cement plant placed in Şanlıurfa, Turkiye. These systems were steam Rankine cycle and organic Rankine cycle and analyzed on energy, exergy and exergoeconomic issues. The organic Rankine cycle performed better exergy efficiency at 63% compared to the Rankine cycle with 53%. However, from an economic point of view, the Rankine cycle is preferable (payback period of 4.738 years) to the Organic Rankine cycle (payback period of 5.074 years). The study of Atmaca, Kanoglu, and Gadalla (2012) aims to achieve an effective energy management of a cement plant located Gaziantep, Turkiye. Energy and exergy analysis were performed on the pyroprocessing unit, and the efficiencies were obtained as 52.2% and 35.9%, respectively. To decrease the amount of heat loss, an insulation system is integrated into the pyroprocessing unit. Thus, both the energy and exergy efficiencies were raised to 63.6% and 47.3%, respectively. By utilizing the waste heat with the waste heat recovery steam generator, electricity is generated and 8.2% of the CO_2 emission is reduced. John proposes that evaluating the cement industry is challenging because of the complicated reactions that took place. Likewise, these reactions are crucial for energetic, exergetic and economic issues. So, the author used process simulations for the analysis. A cement facility located in Tanzania is used as a case study. The outcomes (energy, environment, system behavior) of changing rotary kiln parameters were examined. The simulations were performed by using Aspen Plus software. According to the results, by considering exhaust gases, fuels could be saved, and production costs could be reduced (John 2020).

Research about energy and exergy analysis of pyrolysis of various feedstocks were examined below. In the study of Ismail and Dincer, the multigenerational waste-to-energy system designed for syngas production was analyzed thermodynamically. Aspen Plus and Engineering Equation Solver software were used for the simulation. Energy and exergy analyses were conducted for a detailed analysis. As a result, 55.85% and 43.04% energy and exergy efficiencies were stated, respectively (Ismail and Dincer 2023). Peters et al. conducted an exergy analysis using Aspen Plus. The analyses covered a fast pyrolysis plant that produces crude bio-oil from biomass (hybrid poplar woodchips). The overall exergy efficiency was calculated as 71.2% (Peters, Petrakopoulou, and Dufour 2014). Zhang et al. (2020) studied the pyrolysis of plastic wastes in a rotary kiln to produce gas, oil and char. Then, energy and exergy analysis were implemented in the pyrolysis process using experimental values. The results were 60.9-67.3% and 59.4-66.0% for energy and exergy efficiencies, respectively. In the study of Ebrahimi and Houshfar (2022), thermodynamic analysis was made for an integrated system of anaerobic digestion and pyrolysis. MATLAB and Aspen Plus were used for the analysis. Exergy efficiency was found to be 45.71% for the integrated plant. However, exergy efficiencies resulted in 27.6% and 88.71% for pyrolysis and anaerobic digestion, respectively. In the study of Atienza-Martínez et al. (2018), researchers conducted energy and exergy analysis for three types of thermochemical treatment of sewage sludge. The calculations were made using experimental data. Exergy efficiency results range from 82.3% to 87.8% for torrefaction, 83% for pyrolysis, 73.3% for pyrolysis combined with catalytic post-treatment of the vapors. Li et al. 2024) studied a solar-enhanced biomass pyrolysis system using Aspen Plus. Then, energy and exergy analysis were assessed. As a result, the energy and exergy efficiencies were found as 90.81% and 76.51%, respectively for SCCP (Solar Char-Cycling Pyrolysis). Parvez et al. (2019) compared conventional and microwave-assisted pyrolysis of biomass (gumwood) using thermodynamic assessment. Pyrolysis products, which are gas, char and oil were evaluated in energetic and exergetic ways. Energy and exergy rates resulted in 23% and 26%, respectively, for gas products derived from microwave pyrolysis. Temireyeva, Sarbassov, and Shah (2024) studied slow and fast pyrolysis of biomass (flax straw) using Aspen Plus. In addition, energy and exergy analyses were conducted. Exergy efficiency for slow pyrolysis was in the range of 87-95% and for fast pyrolysis, it ranged from 89% to 98%. In the study of Cruz et al. (2023), thermodynamic analysis was performed for the thermochemical degradation of polypropylene. The results were obtained using experimental data, which were 43% and

38% for energy and exergy efficiencies, respectively. Liu et al. (2018) studied a polygeneration system to obtain lignite and electricity as products. Thermodynamic analyses were applied, and energy and exergy efficiencies were found as 50.21% and 45.41%, respectively. In the study of Sivaraman et al. (2023), researchers studied pyrolysis of Sesamum indicum crop residue. The thermodynamics and sustainability analysis were performed, and energy and exergy efficiencies were found to be 71.2% and 87.3%, respectively.

Hydrogen energy is one of the sustainable energy sources. Since it does not emit gases when burned, it has less environmental impact than conventional energy sources like coal. There are various hydrogen production methods, such as water splitting, biomass conversion, and methane steam reforming. For large scale hydrogen production, PEM electrolysis is a viable method because its maintenance is easy and more environmentally friendly (Ahmadi et al. 2013).

In the study of Ahmadi et al. (2013) a system that combines solar-enhanced PEM electrolyzer with ocean thermal energy conversion system was modeled. The overall system's energy and exergy efficiencies were obtained as 3.6% and 22.7% respectively. However, the exergy efficiency of the PEM electrolyzer was only found to be 56.5%. Fakehi, Ahmadi, and Mirghaed (2015) investigates a hybrid renewable energy system that includes wind energy, electrolyzer and PEM fuel cell. The electrolyzer and fuel cell exergy efficiencies were found to be 68.5% and 47%. Factors like membrane thickness and pressure were determined to be the factors affecting efficiencies. In the study of production El Jery et al. (2023) a PEM electrolyzer powered with solar energy was studied. Properties like radiation density and current density were investigated to observe the effect on the performance of hydrogen production. Increasing the intensity of solar radiation leads to a decrease in total energy efficiency and an increase in hydrogen. Musharavati et al. (2021) carries out the exergy performance evaluation of geothermal energy powered PEM electrolyzer. Overall energy and exergy efficiencies of the system were found to be 41% and 50%, respectively. The study of Nafchi et al. (2019) discusses the performance of a PEM electrolyzer and the effects of parameters like membrane thickness, current density, temperature and cathode pressure on the energy and exergy efficiency of the electrolyzer. Increasing the temperature and decreasing the cathode pressure led to a decrease in electrolyzer voltage and elevated the energy and exergy efficiency of the electrolyzer. Lower membrane thickness increases the energy and exergy

efficiency. The study of Nejadian et al. (2023) compares three hydrogen production methods (SOEC, PEM and alkaline electrolyzer). Their exergy efficiencies were obtained as 13.15%, 13.04% and 12.41% respectively in exergy-economic optimum conditions. Ni et. al. conducts a parametric study to observe the effects of operating temperature, current density and electrolyte thickness on characteristics of PEM electrolyzer. The energy and exergy efficiencies were found to be nearly the same since the electrical energy is the only energy input. The highest energy efficiency was obtained with high operating temperature and thin electrolytes (Ni, Leung, and Leung 2008).

Literature studies indicate that most of the studies mainly focus on the systems separately. In addition, there was no study that analysis energy and exergy efficiency of waste wind turbine pyrolysis. To address the related gap in the literature, we studied energy and exergy analysis of cement production combined with wind turbine pyrolysis and gas turbine. Furthermore, hydrogen production with cement production was proposed to investigate whether it is applicable.

CHAPTER 3

METHODOLOGY

In this study 2 possible renewable integrations were evaluated to increase efficiency of cement production and to decrease specific energy consumption and CO_2 emissions. Description of systems/ processes particularly and modeling of scenarios was presented in this chapter.

3.1. Description of Systems

3.1.1. Base Scenario: Conventional Cement Production

The basic process scheme of base scenario can be seen in Figure 4. In this scenario, the cement process of the study of Atmaca & Yumrutaş (2014) was considered. Instead of showing all units one by one, the overall process is shown. Besides, the calculations were conducted with consideration of the overall process. Net mass and energy inputs/outputs were shown as a single unit as inlets raw materials, coal, electrical power and air enter the overall cement process. At the outlet, finished cement products, exhaust gases, air leakages, and heat losses took place. The coal was used to supply the heat required for the rotary kiln. The electrical power was the total electricity provided to the entire cement process. Besides, hot gas exhaust streams could be utilized to sustain energy to the system. In other scenarios, it has been examined how this energy need can be met by integrating various systems as pyrolysis, gas turbine and electrolysis.

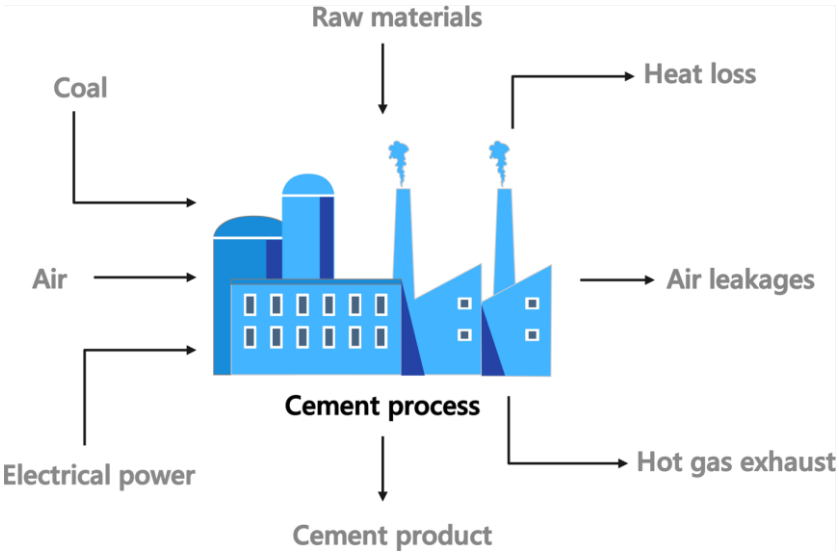

Figure 4. Basic schematic of cement process (scenario 1).

3.1.2. Scenario 1: Cement Process Integrated into Pyrolysis Process and Gas Turbine

In the 1st scenario, in addition to the cement process, there was pyrolysis reactor and a gas turbine, which is shown in Figure 5. The study of (Xu, Ji, Meng, et al. 2023) was taken as a reference for the pyrolysis process. This process took place in a fixed bed reactor at 550 °C (823 K). Wind turbine blade wastes were used as inlet material and named glass fiber reinforced epoxy. This material was shown in two parts, organic and inorganic, because their thermochemical properties are different from each other. The inorganic part is glass fiber, and the organic part is an epoxy matrix. Nitrogen gas was used as inert gas. The process also requires a heat input. The pyrolysis products were oil, gas, solid residue and char. The solid residue consists of glass fiber material. Glass fiber is not flammable, so it could be obtained straightforwardly unchanged after the pyrolysis process. Those obtained solid residue products could be added into the cement process to supply some of the raw materials that enter the cement process. This is possible because of the composition of the solid residues that are similar to cement process raw materials. The compositions of solid residue are given in Table 1, and the compositions of raw materials entering the cement process are given in Table 2.

Table 1. Compositions of solid residue

	Composition	Weight percentage (%)	Reference
Solid residue	SiO_2	58.54	(Hopper n.d.)
	Al_2O_3	8.48	
	CaO	19.83	
	MgO	4.88	
	Na_2O	0.32	
	K_2O	0.21	
	Li_2O	7.74	

Gas and oil products were obtained from the pyrolysis of epoxy matrix, which is the flammable part of the turbine blade material. Pyrolysis oil was entered into the Brayton cycle to obtain electricity. Pyrolysis gas could benefit as additional energy for the system because of its energy content. Besides, hot gas exhaust emerges from cement process could be utilized to obtain additional heat source. Combustion product stream exits from air preheater was also considered as potential heat source. Thus, a preheating system was integrated to scenario 1. It was aimed to eliminate the dependency of grid electricity and use coal as heat source.

The new version of scenario 1 was shown in Figure 6. Pyrolysis gas, exhaust gas and combustion products were used as hot streams into preheaters. In preheater 1 (P-1) waste blades were heated with hot combustion product stream before entering the pyrolysis reactor. With hot pyrolysis gas waste blades were heated one more time in second preheater (P-2). Then waste turbine blade materials were fed to the reactor. By this way, the heat required for pyrolysis reactor was decreased. The gas that emerges from P-2 was still hot, so it was combusted to sustain heat to cement process. So, the required coal amount was reduced.

Calcination reaction took place at 950 ^oC and coal was the heat source used to raise the temperature to this level. To decrease the amount of coal combusted, $CaCO_3$, which is the subject of calcination reaction was preheated. For this reason, some part of the raw material (limestone and marl) was entered into preheater 3 (P-3). Since their $CaCO_3$ composition was about 99wt%. Hot gas exhaust released from cement process

was combined in a mixer then fed to the P-3 to heat limestone and marl, finally released to the atmosphere. Then that part of the cement raw material was heated one more time in preheater 4 (P-4) after that entered to cement process. Hot stream of P-4 was combustion product emerges from P-1 and then discharged to the atmosphere.

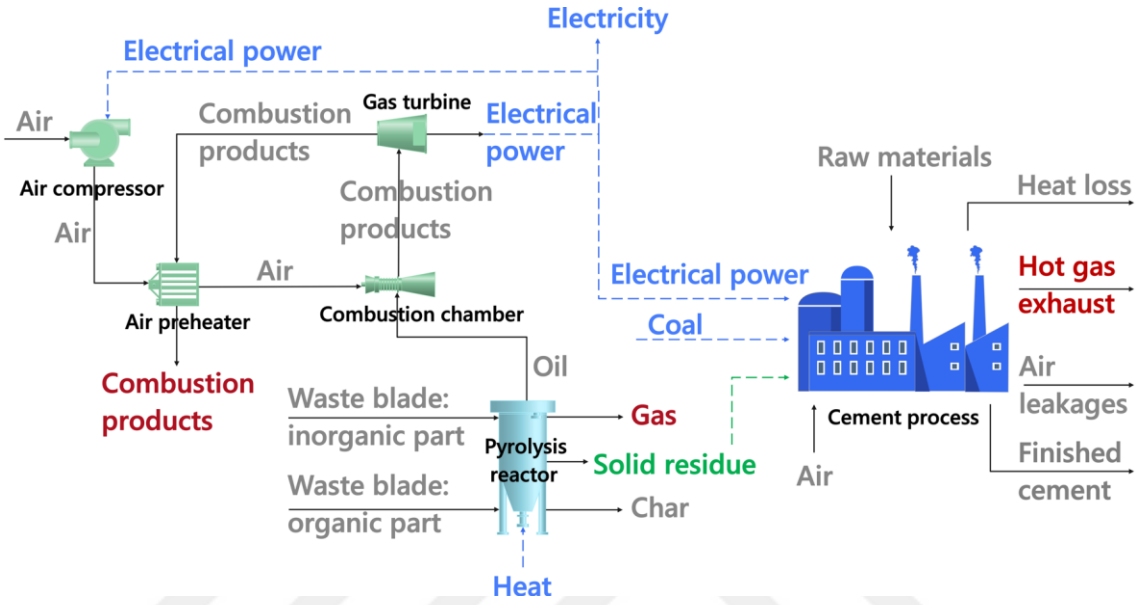

Figure 5. Basic schematic of cement process integrated into pyrolysis process and gas turbine (scenario 1).

The Brayton cycle was used to generate power through the gas turbine. In that scenario, electricity was produced with the help of a gas turbine fueled with pyrolysis oil. In the air compressor, inlet air was compressed isentropically, and compressed air enters the air preheater. Pyrolysis oil was combusted with the air to produce combustion products. These combustion products run the gas turbine to produce electricity. Then, the produced electricity was provided to the cement process to meet its electrical requirements. If the electricity produced was more than electricity required for cement process, this electricity could be supplied to air compressor. Hot combustion products were sent to the air preheater to cool down a little. Furthermore, the outlet combustion products could be utilized to sustain further energy to the system.

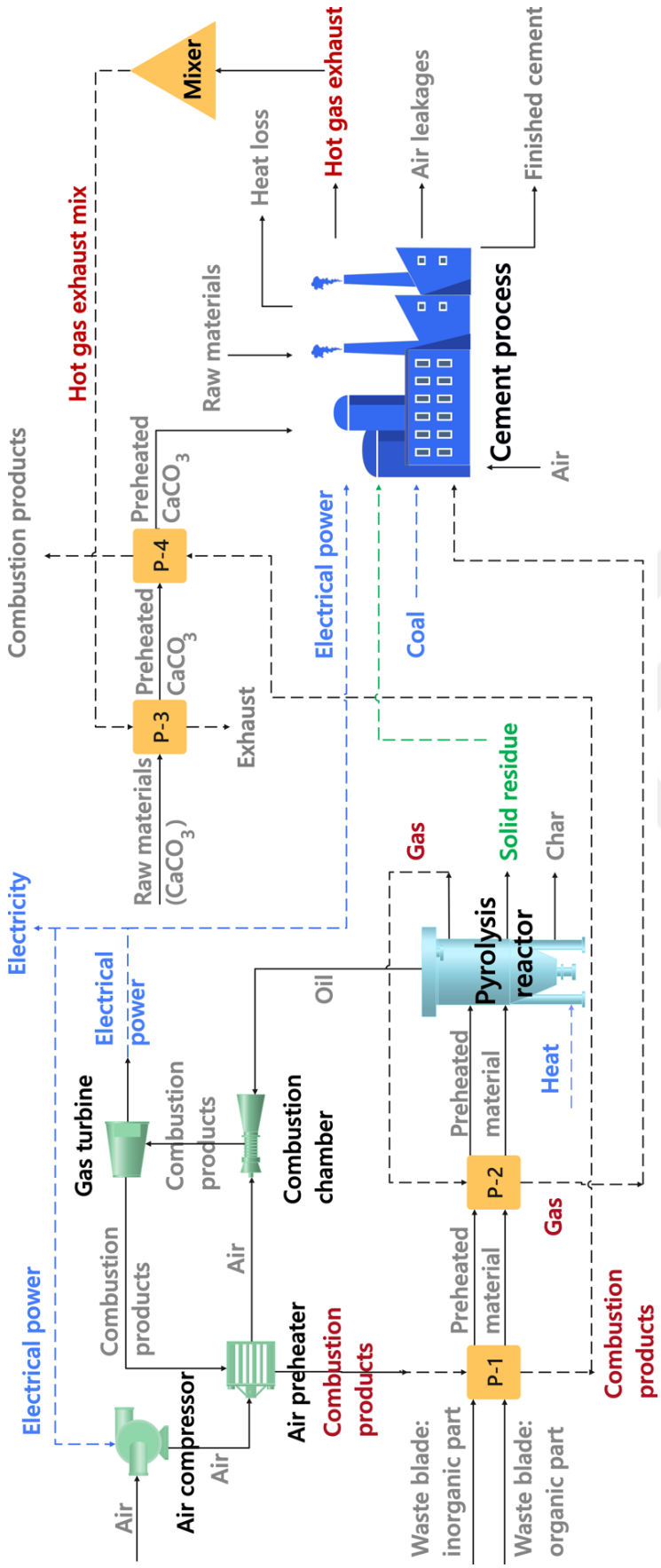

Figure 6. Basic schematic of scenario 1 with preheating.

3.1.3. Scenario 2: Electrolyzer Integrated into Cement Process

Figure 7 illustrates scenario 2. In this scenario, an electrolysis unit was included to the base scenario. The aim here was to use the hydrogen produced from electrolysis to provide heat instead of coal in the cement. The hydrogen was combusted in rotary kiln to supply required heat to the system. Water enters the electrolyzer, and then oxygen and hydrogen gas were obtained as products. The hydrogen produced was replaced with coal and met all the heat needed. In this scenario, no coal was used, and this has many advantages in terms of the environment. However, it creates a negative economic situation. Because the electrolysis unit requires a lot of power, this situation could be examined in more detail by analyzing the energy and exergy efficiency, as well as environmental and economic analysis.

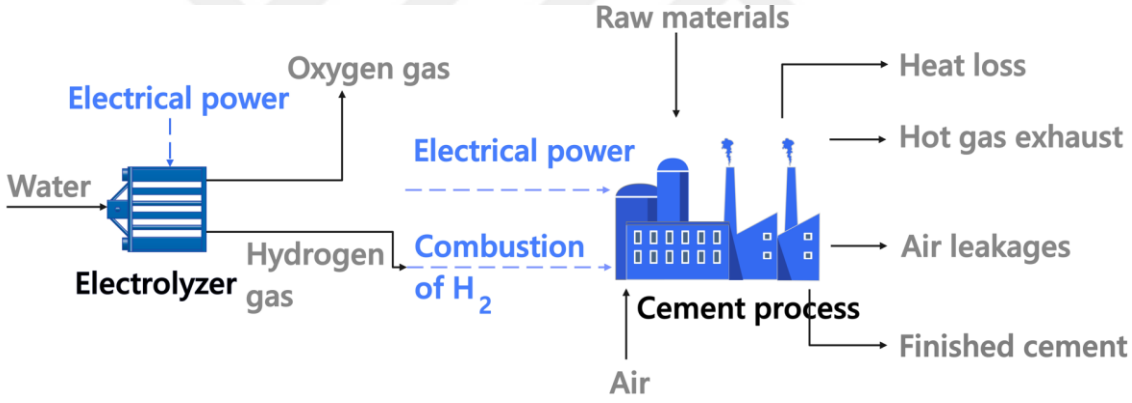

Figure 7. Basic schematic of electrolyzer integrated into cement process (scenario 2).

3.2. Modeling Approach

In this part the steps of the mathematical modeling process were described. First, the system was modeled using EES Software. Then, energy and exergy calculations were performed for each process and overall system. Assumptions made for modeling the system was given as follow.

Assumptions

- The feedstock amount of the pyrolysis process was assumed as 500 kilotons per year according to predictions by year 2050 (Liu and Barlow 2017).
- Pyrolysis temperature was chosen as 823 K.
- Inert N_2 gas was disregarded in the calculations.
- Cement process was considered as a single unit (considering all details regarding process units in cement process) (Atmaca 2014)
- Electrolyzer type and temperature was chosen as PEM electrolyzer and 70 ºC, respectively.
- Reference temperature and pressure were 298 K and 101.3 kPa, respectively.

3.2.1. Cement Process

The study of Atmaca and Yumrutaş (2014) was used as reference for the cement process. In this study, energy and exergy analysis was performed for a cement plant located in Gaziantep, Turkiye. 46 inlet and outlet streams were demonstrated, including raw materials, coal, electrical power, heat losses, air leakages, exhaust gases, intermediate products, and final cement products. Schematic of overall process was given in Figure 8 and their streams was supplied in Table 15 in Appendix A.

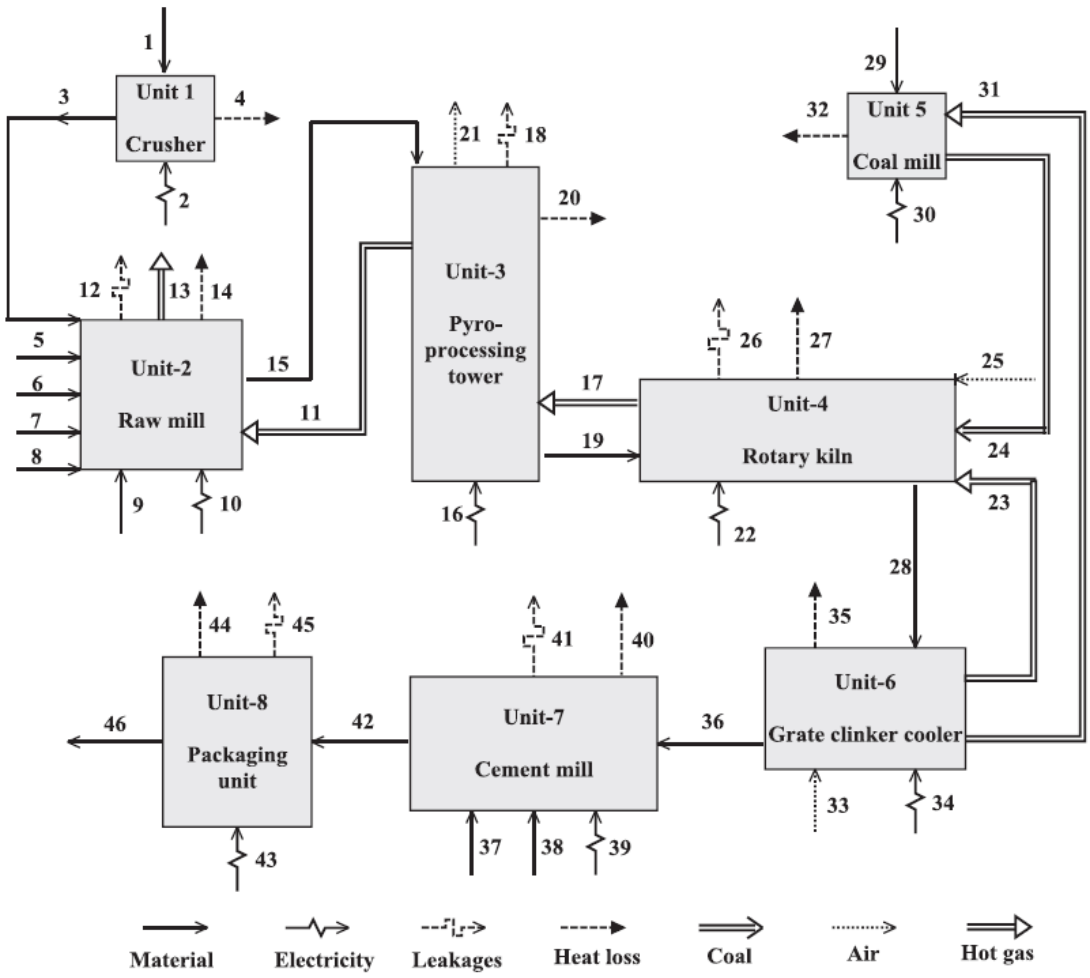

Figure 8. The schematic of reference cement manufacturing plant (Source: Atmaca and Yumrutaş 2014).

The boundary of this cement facility was decided as overall process. Intermediate streams were not included, and net inlet/outlet streams were defined to be used in calculations. Raw material streams (1-8) include limestone, marl, clay, iron ore, bauxite, moisture, gypsum and limestone. Each of the components consists of different compositions. These compositions were given in Table 2 with their references.

Table 2. Compositions of the raw materials entering the cement process

Stream #	Component	Composition	Weight percentage (%)	References
1	Coarse limestone	$CaCO_3$	100	-
2	Marl	$CaCO_3$ SiO_2 Al_2O_3 Fe_2O_3 MgO	96.21 2.32 0.72 0.38 0.37	(Benjatikul, Mahamongkol, and Wongtrakul 2020)
3	Clay	SiO_2 Al_2O_3 Fe_2O_3 CaO MgO Na_2O K_2O $CaCO_3$ $MgCO_3$	71.81 13.37 5.28 0.46 0.91 0.45 1.46 0.63 0.74	(Šveda and Sokolář 2013)
4	Iron ore	Fe_2O_3	100	-
5	Bauxite	Al_2O_3 Fe_2O_3 CaO SiO_2 TiO_2	53 4.5 2.7 1.7 2.4	(Rao et al. 1997)
6	Moisture	H_2O	100	-
7	Gypsum	$CaSO_4$	100	-
8	Limestone	$CaCO_3$	100	-

The coal was used to supply heat to the rotary kiln, where most of the reactions take place. The type of coal used was lignite coal, and its compositions were given in Table 3, along with the heating values of lignite coal.

Table 3. Compositions and heating values of lignite coal

Component	Weight percentage (%)	References
Moisture	30-34	(Atmaca 2014)
Sulfur	0.6-1.6	
Ash	7-16	
Heating values		
HHV (MJ/kg)	**LHV (MJ/kg)**	
-	31.1	

The properties of all streams of the cement process were given in Table 4.

Table 4. Mass flow rates, temperatures, enthalpy and exergy rates of cement process in base scenario

Stream #	Stream name	ṁ (kg/s)	T(K)	Energy rate (kJ/s)	Exergy rate (kJ/s)
1	Limestone	20.62	298.20	0.00	1041.00
2	Marl	12.01	298.20	0.00	761.20
3	Clay	4.13	298.20	0.00	1750.00
4	Iron ore	0.37	298.20	0.00	47.11
5	Bauxite	0.37	298.20	0.00	644.60
6	Moisture	4.17	298.20	0.00	2199.00
7	Gypsum	0.92	298.20	0.00	29.12
8	Limestone	0.99	298.20	0.00	49.79
9	Coarse coal	2.00	298.20	62200.00	68743.00
10	Primary air	2.74	298.20	0.00	9.73
11	Fresh air	47.00	298.20	0.00	166.80
12	Exhaust	18.43	523.00	4222.00	1141.00
13	Hot gas exhaust	37.10	380.00	3263.00	4654.00

(cont. on next page)

Table 4 (cont.)

14	Air leakages	1.13	298.20	0.00	4.00
15	Air leakages	7.01	300.00	13.04	24.90
16	Air leakages	3.58	710.00	1006.00	5949.00
17	Air leakages	1.14	381.00	95.48	15.28
18	Air leakages	0.10	310.00	13.62	4.32
19	Hot gas exhaust	4.97	707.00	2222.00	1379.00
20	Cement product	20.79	310.00	164.90	5871.00
21	Electrical power	-	-	18782	18782
22	Heat loss	-	-	69981.96	69981.96

3.2.2. Pyrolysis Process

The pyrolysis process was established according to the study of Xu, Ji, Meng, et al. (2023). The study investigates the pyrolysis of GFRP (glass fiber reinforced polymer) part of the retired turbine blades. The blades were taken from an industrial wind farm located in China. The experiments were conducted at temperatures 400, 450, 500, 550 and 600 ºC. For this thesis, 550 ºC (823 K) was selected, however a parametric analysis could be made as a further study at various temperatures. The experiments were performed in a fixed bed reactor under N_2 atmosphere. The amount of GFRP to be fed to the reactor was decided according to the wind turbine blade waste amounts. According to Liu and Barlow (2017) global waste amount will reach 2 million tones in 2050. Besides, Europe will consist of 25% of this waste amount. It was assumed that, all the waste blade

around the Europe will be fed to the cement facility. Therefore 500,000 tones/year of waste blade amount was subjected to the pyrolysis process.

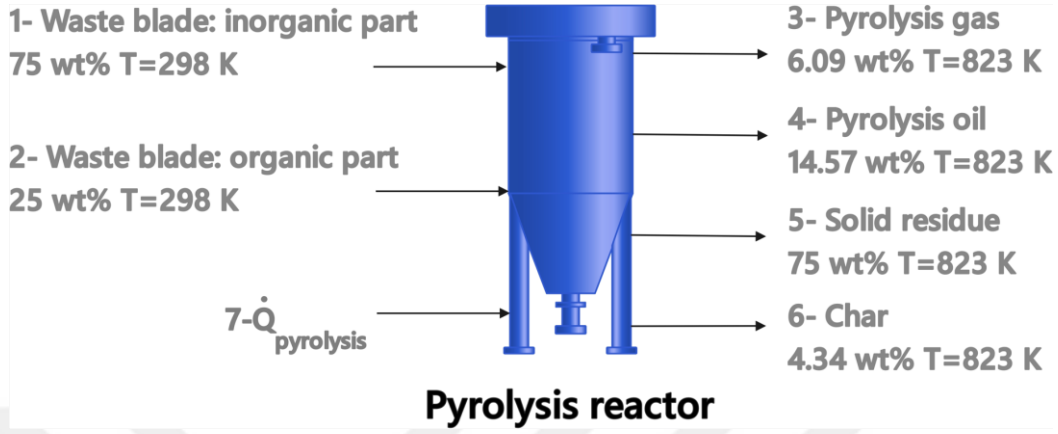

Figure 9. Basic schematic of pyrolysis process.

The GFRP pieces entered the reactor and as products pyrolysis gas, pyrolysis oil, solid residues and char were obtained. The basic schematic of the pyrolysis process can be seen in Figure 9 and properties of the streams can be seen in Table 5.

Table 5. Properties of pyrolysis streams

Stream #	**Stream name**	**Weight percentage (%)**	**T(K)**
1	Fiberglass	75	298
2	Epoxy matrix	25	298
3	Pyrolysis gas	6.09	823
4	Pyrolysis oil	14.57	823
5	Solid residue	75	823
6	Char	4.34	823
7	$\dot{Q}_{pyrolysis}$	-	-

In the schematic, GFRP was demonstrated as 2 parts which are fiberglass part (inorganic part) and polymer part (organic part). The fiberglass is the uncombusted part which obtained as solid residue as product. Those parts were added to cement facility as

raw material. Other than solid residue, there was char product as well. The pyrolysis streams and their compositions can be seen in Table 6.

Table 6. Compositions of pyrolysis process streams

Stream #	Stream name	Compositions	Weight Percentage (%)
5	Waste blade: inorganic part	SiO_2	58.54
		Al_2O_3	8.48
		CaO	19.83
		MgO	4.88
		Na_2O	0.32
		K_2O	0.21
		Li_2O	7.74
6	Waste blade: organic part	*$CH_{1.38}O_{0.33}$	100
7	Pyrolysis gas	H_2	0.43
		CH_4	32.55
		CO	23.21
		CO_2	31.14
		C_2H_4	4.82
		C_2H_6	7.84
8	Pyrolysis oil	*$CH_{1.69}O_{0.44}$	100
9	Solid residue	SiO_2	58.54
		Al_2O_3	8.48
		CaO	19.83
		MgO	4.88
		Na_2O	0.32
		K_2O	0.21
		Li_2O	7.74
10	Char	C	100

*Normalized chemical formulas were calculated

3.2.3. Brayton Cycle

The Brayton cycle is a thermodynamic cycle that is used for power generation from gas turbines and shown in Figure 10 (Guo et al. 2024). It converts thermal energy into mechanical energy (Ancona et al. 2024). The equipment used for the Brayton cycle in this study were air compressor, air preheater, combustion chamber and gas turbine. At first, fuel (pyrolysis oil) entered the combustion chamber. Air was first compressed in air compressor and sent to the air preheater. Then, heated air was combusted with fuel in the combustion chamber. Combustion products left the combustion chamber and entered the gas turbine. Electricity was produced here, and combustion products entered the air preheater to decrease its temperature.

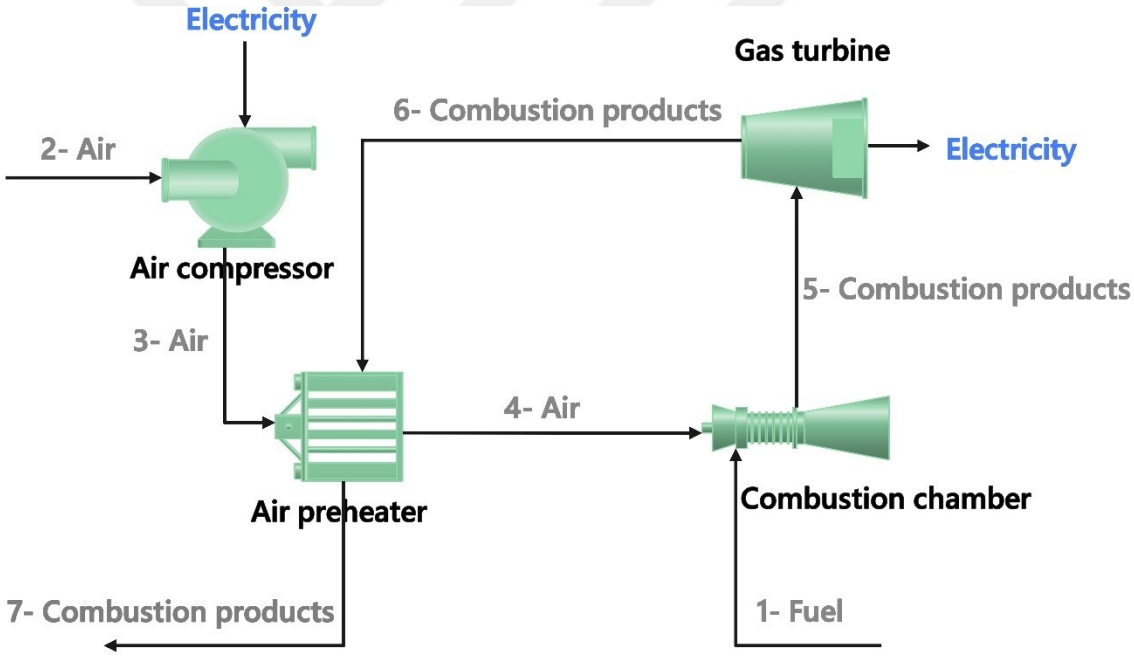

Figure 10. Basic schematic of Brayton cycle.

Brayton cycle was used in scenario 1. In that scenario, the fuel that entered the combustion chamber was pyrolysis oil. The operating temperature of the pyrolysis reactor was 823 K (550 ºC), so outlet pyrolysis oil temperature was 823 K.

The air amount that will enter the combustion chamber was determined according to the fuel composition. It was calculated due to $\bar{\lambda}$ which is fuel to air ratio and defined as (Hajimohammadi Tabriz et al. 2024);

$$\bar{\lambda} = \frac{\dot{n}_F}{\dot{n}_a} \tag{1}$$

For scenario 1, in the combustion chamber, the pyrolysis oil reacts with air. The reaction of pyrolysis oil and air is given as follow;

$$\bar{\lambda}[Fuel] + [0.7748N_2 + 0.2059O_2 + 0.0003CO_2 + 0.019H_2O] \rightarrow [1 + \bar{\lambda}][Y_{N_2}N_2 + Y_{O_2}O_2 + Y_{CO_2}CO_2 + Y_{H_2O}H_2O] \tag{2}$$

The fuel composition given as: 0.32C+0.54H+0.14O, which is the pyrolysis oil found by mole fractions of elements.

The following equations are written according to the molar balance of components in the general oil combustion reaction:

$$Y_{CO_2} = \frac{\bar{\lambda}(0.32) + 0.0003}{1 + \bar{\lambda}} \tag{3}$$

$$Y_{H_2O} = \frac{\bar{\lambda}(0.27) + 0.019}{1 + \bar{\lambda}} \tag{4}$$

$$Y_{O_2} = \frac{\bar{\lambda}(-0.385) + 0.2059}{1 + \bar{\lambda}} \tag{5}$$

$$Y_{N_2} = \frac{0.7748}{1 + \bar{\lambda}} \tag{6}$$

The energy balance for the combustion chamber, assuming that the heat loss is 2% of the LHV of the fuel, is written as follows:

$$0 = -0.02\overline{\lambda LHV} + \bar{h}_8 + \bar{\lambda}\bar{h}_4 - (1 + \bar{\lambda})\bar{h}_9 \tag{7}$$

Therefore, $\bar{\lambda}$ is expressed as:

$$\bar{\lambda} = \frac{0.7748\Delta\bar{h}_{N_2} + 0.2059\Delta\bar{h}_{O_2} + 0.0003\Delta\bar{h}_{CO_2} + 0.019\Delta\bar{h}_{H_2O}}{\bar{h}_4 - 0.02\overline{LHV} - (0.32\bar{h}_{CO_2} + 0.27\bar{h}_{H_2O} - 0.385\bar{h}_{O_2})_{(T_9)}} \quad (8)$$

$\overline{LHV}$ is given as:

$$\overline{LHV} = \bar{H}_{prod} - \bar{H}_{react} = \sum N_p \bar{h}^0_{f,p} - \sum N_r \bar{h}^0_{f,r} \quad (9)$$

Compositions of the Brayton cycle for scenario 1 were given in Table 7 according to stream numbers shown in Figure 10.

Table 7. Compositions of Brayton cycle streams for scenario 1

Stream #	**Stream name**	**Compositions**	**Mole percentages (%)**
1	Pyrolysis oil	C	31.98
		H	53.96
		O	14.06
2, 3, 4	Air	N_2	77.48
		O_2	20.59
		CO_2	0.03
		H_2O	1.9
5, 6, 7	Combustion products	N_2	74.48
		O_2	18.30
		CO_2	1.27
		H_2O	2.88

3.2.4. PEM Electrolyzer

A PEM electrolyzer has a polymeric membrane that conducts protons and insulates electrons. It also contains electrodes, an anode, and a cathode where oxygen and hydrogen are produced. The electrolyzer uses electricity to convert water into hydrogen

and oxygen (Falcão and Pinto 2020). At the anode Oxygen Evolution Reaction (OER) occurs as follows;

$$H_2O \rightarrow 2H^+ + \frac{1}{2}O_2 + 2e^- \tag{10}$$

Then the membrane lets H^+ ions (protons) to pass through to the cathode. At the cathode Hydrogen Evolution Reaction (HER) occurs as follows;

$$2H^+ + 2e^- \rightarrow H_2 \tag{11}$$

When these two reactions combined, the global reaction becomes;

$$H_2O \rightarrow H_2 + \frac{1}{2}O_2 \tag{12}$$

The produced hydrogen mole flow rate is calculated with the following formula;

$$\dot{n}_{H_2} = \frac{I_{PEM}}{2F} \tag{13}$$

Where I_{PEM} is current with a unit of Ampere (A). F is Faraday's constant equal to 96485 C/mol (A.s/mol). C is coulomb which is electric charge unit. 2 is defined as the number of electrons exchanged per molecule of hydrogen.

The produced oxygen mole flow rate is found with equation given;

$$\dot{n}_{O_2} = \frac{I_{PEM}}{4F} \tag{14}$$

Where 4 is the number of electrons exchanged per molecule of oxygen.

The required electrical power for PEM electrolyzer is found by formula given;

$$\dot{W}_{PEM} = I_{PEM} * V_{PEM} \tag{15}$$

Where V_{PEM} is the PEM electrolyzer voltage in a unit of V. The PEM electrolyzer voltage was specified between 1.8 V and 2.2 V (Millet and Grigoriev 2014), (Ozdemir et al. 2024) 2.0 V of voltage value was selected for this study. However, a parametric study could be conducted while choosing the optimum value.

In this study, a PEM electrolyzer was used to produce hydrogen. Water enters the electrolyzer and forms hydrogen and oxygen gases. Oxygen is released into the atmosphere, and hydrogen is incorporated into the system in different ways to sustain energy. In scenario 2, hydrogen gas was directly burned in the rotary kiln of the cement process and replaced with coal. Besides producing energy with hydrogen, the electrolysis unit itself requires energy that was denoted as $\dot{W}_{PEM}$ and shown in Figure 11 in the basic schematic of PEM electrolyzer. This energy was supplied with electricity. The operating temperature for PEM electrolyzer ranges between 60 ºC and 80 ºC according to literature (Ma et al. 2024). 70 ºC was selected as the operating temperature. However, a parametric study could be maintained for deciding the best option

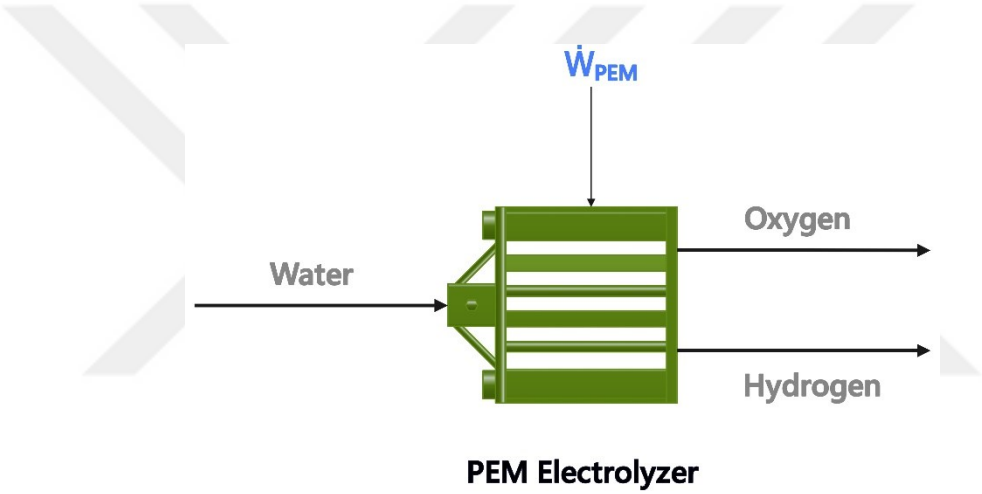

Figure 11. Basic schematic of PEM electrolyzer.

The system inputs and outputs for electrolyzer unit are given in Table 8 for scenario 2.

Table 8. PEM electrolyzer inputs and outputs for scenario 2

		ṁ (kg/s)	**Power (kW)**
Input	Water (H_2O)	4.63	-
	$\dot{W}_{peme}$	-	99,228
Output	H_2	0.52	-
	O_2	4.11	-

3.3. Energy Analysis

The 1st law of thermodynamics was considered while performing energy analysis. The laws of conservation of mass and energy were applied to all the systems.

Mass balance equation was given as;

$$\sum_i \dot{m}_i = \sum_o \dot{m}_o \tag{16}$$

Energy balance of the system can be written as;

$$\sum_i E_i = \sum_o E_o \tag{17}$$

$$\sum_j \dot{Q}_j + \sum_i \dot{m}_i h_i = \dot{W} + \sum_o \dot{m}_o h_o \tag{18}$$

Total energy on a unit molar basis is given as;

$$en = en_{ph} + en_{ch} + en_{ke} + en_{pe} \tag{19}$$

Where en_{ph}, en_{ch}, en_{ke}, en_{pe} are physical, chemical, kinetic and potential energies, respectively. Kinetic and potential exergies were considered negligible, since we assume the system at rest relative to the environment (Wang et al. 2016).

Thus, the energy equation has become;

$$en = en_{ph} + en_{ch} \tag{20}$$

The physical energy is defined as;

$$en_{ph} = h - h_0 \tag{21}$$

$$h - h_0 = \int C_p dT \tag{22}$$

The chemical energy is defined as;

$$en_{ch} = LHV_i * MW_i * 1000 \quad (23)$$

where LHV is the lower heating value and has a unit of MJ/kg. Calculation of LHV was explained in 3.4. Exergy Analysis part.

3.3.1. Energy Efficiency

Energy efficiency of a system is useful energy output divided by energy input and defined as follows;

$$Energy\ efficiency\ \% = \frac{useful\ energy\ output}{energy\ input} * 100 \quad (24)$$

The energy efficiency of scenarios was given for each unit as follows;

Base scenario:

Overall/ Cement process:

$$\eta_{cement} = \frac{\dot{Q}_{cement} + \dot{n}_{exhaust} en_{exhaust}}{\dot{m}_{coal} LHV_{coal} + \dot{W}_e} * 100 \quad (25)$$

$\dot{W}_e$ is the electrical power required for cement process. $\dot{Q}_{cement}$ defines the energy output caused by the reactions take place during cement production. Reactions occurring in cement process was given as;

$$Reaction\ 1: CaCO_3 \rightarrow CaO + CO_2 \quad \Delta\hat{h}^o_{rxn,1} = 178327\ kJ/kmol \quad (26)$$

$$Reaction\ 2: 2CaO + SiO_2 \rightarrow Ca_2SiO_4 \quad \Delta\hat{h}^o_{rxn,2} = -65090.5\ kJ/kmol \quad (27)$$

$$Reaction\ 3: 3CaO + SiO_2 \rightarrow Ca_3SiO_5 \quad \Delta\hat{h}^o_{rxn,3} = -37692.7\ kJ/kmol \quad (28)$$

The first reaction is the calcination reaction, the second reaction is belite formation reaction and the third one is alite formation. Belite and alite are intermediate products in cement process and one of the main ingredient for clinker formation.

$\Delta\hat{h}^{o}_{rxn,i}$ defines the heat of reaction and $\dot{Q}_{cement}$ was found as;

$$\dot{Q}_{cement} = \Delta\hat{h}^{o}_{rxn,1}\dot{n}_{CaO} + \Delta\hat{h}^{o}_{rxn,2}\left(\frac{\dot{n}_{CaO}}{2}\right) + \Delta\hat{h}^{o}_{rxn,3}\left(\frac{\dot{n}_{CaO}}{2}\right) \quad (29)$$

<u>*Scenario 1:*</u>

Overall:

$$\eta_{overall} = \quad (30)$$

$$\eta_{overall} = \frac{\dot{Q}_{cement} + \dot{W}_{electricity}}{\dot{m}_{waste}LH\dot{V}_{waste} + m_{coal}LHV_{coal} + \dot{Q}_{pyr}} * 100$$

where $\dot{W}_{electricity}$ was the electricity amount left after electricity produced from gas turbine was supplied to cement process and air compressor and defined as;

$$\dot{W}_{electricity} = \dot{W}_{gt} - \dot{W}_{ac} - \dot{W}_{e} \quad (31)$$

Pyrolysis:

$$\eta_{pyrolysis} = \frac{\dot{m}_{oil}LHV_{oil} + \dot{m}_{gas}LHV_{gas}}{\dot{m}_{waste}LHV_{waste} + \dot{Q}_{pyr}} * 100 \quad (32)$$

Waste subscript was used to define wind turbine blade waste and $\dot{Q}_{pyr}$ is defined the heat required for pyrolysis reactor. Oil and gas was the desired energy content for pyrolysis.

Brayton Cycle:

$$\eta_{brayton} = \frac{\dot{W}_{net} + \dot{m}_{cb}LHV_{cb}}{\dot{m}_{oil}LHV_{oil}} * 100 \quad (33)$$

Subscript “cb” was used to define combustion products emerges from air preheater. Since its outlet temperature was high, it was considered to be utilized. $\dot{W}_{net}$ was defined as the difference between electricity produced from gas turbine and electricity required for air compressor;

$$\dot{W}_{net} = \dot{W}_{gt} - \dot{W}_{ac} \tag{34}$$

Cement process:

$$\eta_{cement} = \frac{\dot{Q}_{cement} + \dot{n}_{exhaust} en_{exhaust}}{\dot{m}_{coal} LHV_{coal} + \dot{m}_{gas} LHV_{gas} + \dot{n}_{CaCO_3} en_{CaCO_3} + \dot{W}_e} * 100 \tag{35}$$

In here $\dot{m}_{gas} LHV_{gas}$ and $\dot{n}_{CaCO_3} h_{CaCO_3}$ terms included to the inlet energy section. Unlike the base scenario, pyrolysis gas was combusted so $\dot{m}_{gas} LHV_{gas}$ was added. $\dot{n}_{CaCO_3} h_{CaCO_3}$ term added because $CaCO_3$ composition was first preheated and then fed to the cement process.

<u>*Scenario 2:*</u>

Overall:

$$\eta_{overall} = \frac{\dot{Q}_{cement} + \dot{n}_{exhaust} en_{exhaust}}{\dot{W}_{PEM} + \dot{W}_e} * 100 \tag{36}$$

$\dot{W}_{PEM}$ was included to the energy efficiency calculation because of energy requirement of PEM electrolysis.

Cement process:

$$\eta_{cement} = \frac{\dot{Q}_{cement} + \dot{n}_{exhaust} en_{exhaust}}{\dot{m}_{H_2} LHV_{H_2} + \dot{W}_e} * 100 \tag{37}$$

In scenario 2 for cement process efficiency, $\dot{n}_{coal} h_{coal}$ was excluded since coal was not used in this scenario. Instead, H_2 was considered.

Electrolysis:

$$\eta_{electrolysis} = \frac{\dot{m}_{H_2} LHV_{H_2}}{\dot{W}_{PEM}} * 100 \tag{38}$$

$\dot{W}_{PEM}$ was considered as the energy inlet to the electrolyzer and energy content of the hydrogen gas was the desired energy content.

3.4. Exergy Analysis

Exergy is defined as the maximum amount of useful work that can be produced by a system as it achieves equilibrium with its surroundings. In other words, it is the quality of energy (Bejan 1995). The 2nd law of thermodynamics is taken into account for exergy balance equation and defined as follows;

$$\sum_j \dot{Q}_j(1-\frac{T_0}{T_j}) + \sum_i \dot{m}_i\, ex_i = \dot{W} + \sum_o \dot{m}_o\, ex_o + \dot{E}x_D \tag{39}$$

In here subscript j denotes the species, inlet and outlet is defined with subscript i and o, respectively. Ex is the exergy of an unit molar.

$\dot{E}x_D$ defines the exergy destruction rate due to irreversibilities and it is found by;

$$\dot{E}x_D = \dot{E}x_{in} - \dot{E}x_{out} \tag{40}$$

Total exergy on a unit molar basis is given as;

$$ex = ex_{ph} + ex_{ch} + ex_{ke} + ex_{pe} \tag{41}$$

Where ex_{ph}, ex_{ch}, ex_{ke}, ex_{pe} are physical, chemical, kinetic and potential exergies, respectively. Kinetic and potential exergies are considered negligible, since we assume the system at rest relative to the environment (Bejan, 1995).

Thus, the exergy equation has become;

$$ex = ex_{ph} + ex_{ch} \tag{42}$$

The physical exergy is defined as;

$$ex_{ph} = (h - h_0) - T_0(s - s_0) \tag{43}$$

$$h - h_0 = \int C_p dT \tag{44}$$

$$s - s_0 = \int C_p dT/T \tag{45}$$

The chemical exergy is defined as;

$$ex_{ch} = \sum y_i \, ex_{0,i} + RT_0 \sum y_i \, ln\gamma_i y_i \tag{46}$$

Where y_i is the molar fraction, $ex_{0,i}$ is standard molar chemical exergy and γ_i is activity coefficient of substances, respectively. The standard molar chemical exergies of substances are obtained from Kotas (Kotas 1985). The activity coefficient is considered as 1, since the gas mixtures are assumed as ideal (Caglar, Tavsanci, and Biyik 2021).

The chemical exergy of the epoxy resin part of the waste turbine blade material is calculated by the following equation;

$$ex_{ch}^{ob} = M_{ob}(LHV_{ob} * 1000 + 2442w)\varphi + 9417s \tag{47}$$

Where M_{ob} is molar mass and LHV_{ob} is the lower heating value of the organic part of the blade material. w is the mass fraction of moisture, s is the mass fraction of sulfur. φ is defined for mass fraction ratio of oxygen to carbon less than 0.667 as;

$$\varphi_{dry} = 1.0437 + 0.1882\frac{h}{c} + 0.0610\frac{o}{c} + 0.0404\frac{n}{c} \tag{48}$$

Where h, c, o and n are the mass fractions of hydrogen, carbon, oxygen and nitrogen, respectively.

Heating value is the measure of thermal energy released when a fuel is burned completely. LHV assumes that water produced during combustion is in vapor form. In addition, there is another type of heating value HHV (higher heating value). HHV assumes that water is in a liquid phase (Wiebren 2015).

LHV is calculated by the following two equations, first one is used to find the LHV of dry base fuel (Wiebren 2015);

$$LHV^{db} = HHV - 2.4 * 8.9Y_H \; [MJ/kg] \tag{49}$$

Thus, there is a difference between LHV and HHV, and it is the latent heat of vaporization of water at the standard temperature of 25 °C (~2.4 MJ/kg).

2.4 MJ/kg is the latent heat of vaporization of water at the standard temperature of 25 °C. It specifies the difference between LHV and HHV. 8.9 kg/kg is the stoichiometric ratio of water to H. Y_H is the mass fraction of H.

The HHV (dry base) can be found by ultimate analysis using following formula (Gaur and Reed, 1995);

$$HHV = 34.91Y_C + 117.83Y_H + 10.05Y_S - 1.51Y_N - 10.34Y_O - 2.11Y_{ash}\ [MJ/kg] \quad (50)$$

Where Y_C, Y_H, Y_S, Y_N, Y_O and Y_{ash} is the mass fractions of carbon, hydrogen, sulfur, nitrogen, oxygen and ash, respectively.

3.4.1. Exergy Efficiency

Exergy efficiency of a system is useful exergy output divided by exergy input and defined as follows;

$$Exergy\ efficiency\ \% = \frac{useful\ exergy\ output}{exergy\ input} * 100 \quad (51)$$

Energy efficiency of scenarios were given for each units as follows;

Base scenario:

Overall/ Cement process:

$$\varphi_{cement} = \frac{\dot{n}_{cement} ex_{cement} + \sum \dot{n}_{exhaust} ex_{exhaust}}{\dot{n}_{coal} ex_{coal} + \sum \dot{n}_{C,in} ex_{C,in} + \dot{W}_e} * 100 \quad (52)$$

Scenario 1:

Overall:

$$\varphi_{Overall} = \frac{\dot{n}_{cement} ex_{cement} + \dot{W}_{electricity}}{\dot{n}_{waste} ex_{waste} + \dot{n}_{coal} ex_{coal} + \sum \dot{n}_{C,in} ex_{C,in} + Ex_{\dot{Q}_{pyr}}} * 100 \quad (53)$$

where $Ex_{\dot{Q}_{pyr}}$ was the exergy of heat of pyrolysis process.

Pyrolysis:

$$\varphi_{pyrolysis} = \frac{\dot{n}_{oil} ex_{oil} + \dot{n}_{gas} ex_{gas}}{\dot{n}_{waste} ex_{waste} + Ex_{\dot{Q}_{pyr}}} * 100 \quad (54)$$

Brayton Cycle:

$$\varphi_{brayton} = \frac{\dot{W}_{net} + \dot{n}_{cb} ex_{cb}}{\dot{n}_{oil} ex_{oil}} * 100 \quad (55)$$

Cement process:

$$\varphi_{cement} = \frac{\dot{n}_{cement} ex_{cement} + \dot{n}_{exhaust} ex_{exhaust}}{\dot{n}_{coal} ex_{coal} + \dot{n}_{gas} ex_{gas} + \sum \dot{n}_{C,in} ex_{C,in} + \dot{W}_e} * 100 \quad (56)$$

<u>*Scenario 2:*</u>

Overall:

$$\varphi_{overall} = \frac{\dot{n}_{cement} ex_{cement} + \dot{n}_{exhaust} ex_{exhaust}}{\sum \dot{n}_{C,in} ex_{C,in} + \dot{W}_{PEM} + \dot{W}_e} * 100 \quad (57)$$

Cement process:

$$\varphi_{cement} = \frac{\dot{Q}_{cement} + \dot{n}_{exhaust} ex_{exhaust}}{\dot{n}_{H_2} ex_{H_2} + \sum \dot{n}_{C,in} ex_{C,in} + \dot{W}_e} * 100 \quad (58)$$

Electrolysis:

$$\varphi_{electrolysis} = \frac{\dot{n}_{H_2} ex_{H_2}}{\dot{W}_{PEM}} * 100 \quad (59)$$

CHAPTER 4

RESULTS AND DISCUSSION

4.1. Base Scenario: Conventional Cement Production

The actual cement facility in the study of Atmaca and Yumrutaş (2014) was used as the base scenario for this study. The overall cement process was accepted as a boundary as seen in Figure 12. The streams between the units in cement facility were not considered for the calculations and only net inlet and outlet streams were demonstrated. So, the energy and exergy analysis were applied to the overall cement production process. Conventional cement production includes raw materials, moisture, coal, air and electrical power as inlet streams. The outlet streams were finished cement products, exhaust gases, air leakages and heat losses.

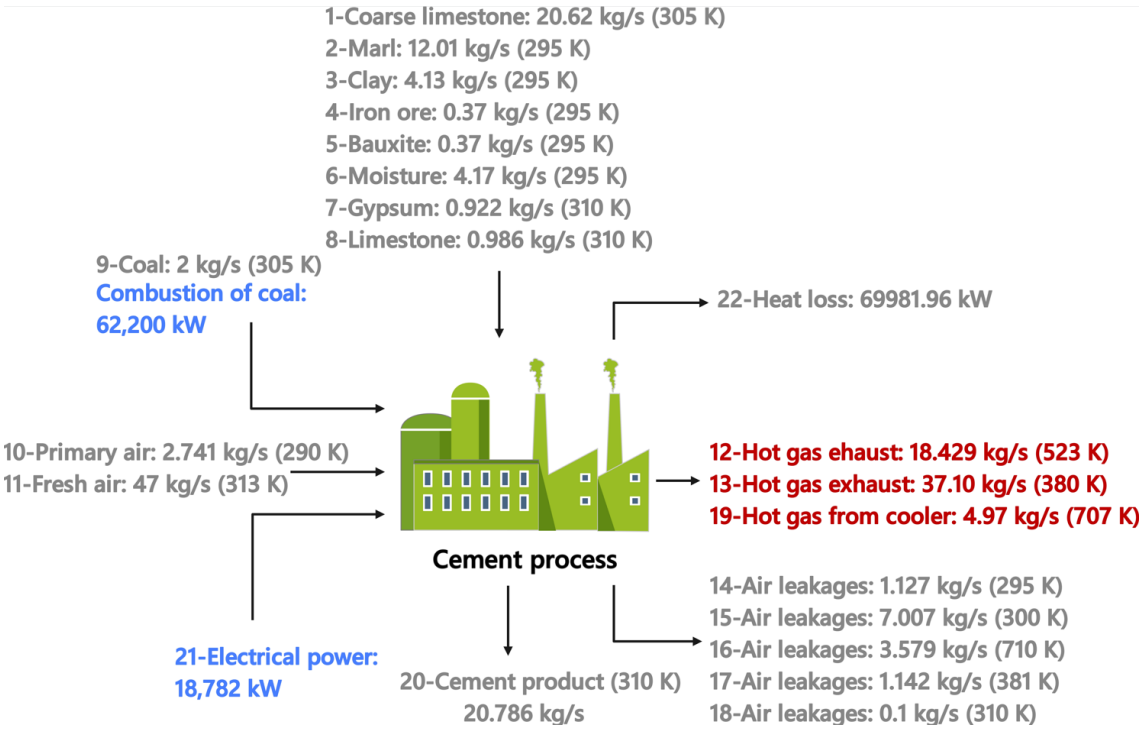

Figure 12. Process schematics of base scenario with results.

The energy efficiency of the cement process was found to be 61.60%, and exergy efficiency was found to be 20.21%, as is given in Table 9. The cement process was integrated with other systems to observe the efficiency variations in other sccenarios.

Table 9. Energy and exergy efficiency results of base scenario

	Energy efficiency (%)	**Exergy efficiency (%)**
Overall	61.60	20.21

4.2. Scenario 1: Cement Process Integrated into Pyrolysis Process and Brayton Cycle with Preheating System

In scenario 1, the pyrolysis process was integrated to sustain energy and raw material to the cement process. Waste wind turbine blade material was used as raw material for the pyrolysis process. Gas, oil and solids were obtained as products. Solid residue product was directed to the cement process to use as raw material. By this way some of the raw materials will be supplied by wind turbine blade wastes. Pyrolysis oil was utilized in the Brayton cycle to produce electricity for the cement process. The electricity produced from the gas turbine was 50707 kW, and the electrical power needed by the cement process was 18782 kW. 26080 kW of electrical power was provided to air compressor and 5845 kW of electrical energy was left. By this way, all of the electricity requirement of the system was sustained by itself. Hot streams which are demonstrated with red in Figure 13 could be utilized to sustain energy to the overall system. Pyrolysis gas stream, combustion products from the Brayton cycle, and hot gas streams from the cement process were the outlet streams that have high temperatures. These hot streams were utilized through preheaters. 4 preheaters were used and they aided to harness the system's excess energy.

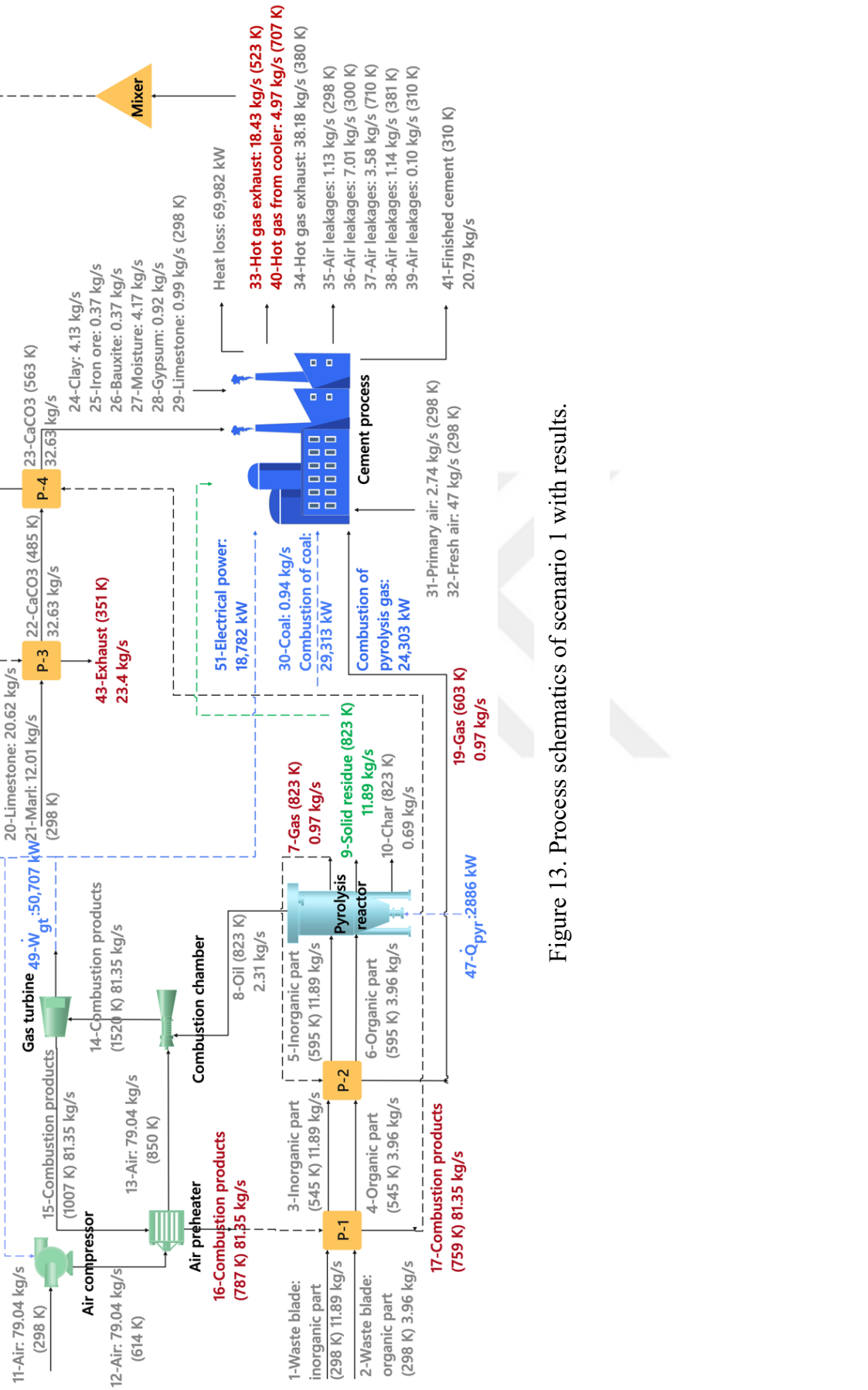

Figure 13. Process schematics of scenario 1 with results.

Under these conditions, energy and exergy efficiencies of the overall system were found to be 35.71% and 15.91%, respectively. For the cement process, the energy and exergy efficiencies were found to be 61.60% and 22.91%, respectively, and the results can be seen in Table 10.

Table 10. Energy and exergy efficiency results of scenario 1

	Energy efficiency	**Exergy efficiency**
Overall	35.71	15.91
Pyrolysis	74.71	77.03
Brayton	84.98	36.98
Cement	61.60	22.91

4.3. Scenario 2: Electrolyzer Integrated into Cement Production

An electrolyzer was integrated into base scenario, as can be seen in Figure 14.

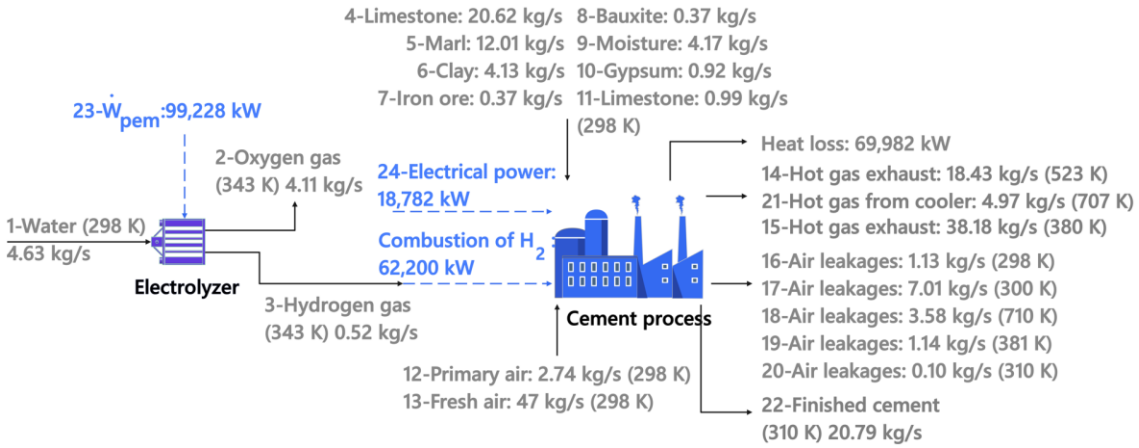

Figure 14. Process schematic of scenario 2 with results.

In this scenario, the energy required for cement was provided by hydrogen energy and the schematic of scenario 1 was given in Figure 11. In cement production 18782 kW of electricity was needed and this energy was supplied by grid electricity same as base scenario. Hydrogen produced by the electrolyzer was directly sent to cement facility to

be combusted. 62,200 kW of energy was obtained which met the energy requirement of cement process. PEM electrolyzer was the another unit that needs electricity which was 99,228 kW.

The energy efficiency of this scenario was found to be 42.27%, and the exergy efficiency was 15.27%. For the cement process, the energy and exergy efficiencies were found to be 61.60% and 21.90%, respectively. Electrolyzer energy efficiency was 62.68%, and exergy efficiency was 61.93%, as can be seen in Table 11.

Table 11. Energy and exergy efficiency results of scenario 2

	Energy efficiency	**Exergy efficiency**
Overall	42.27	15.27
Cement	61.60	21.90
Electrolysis	62.68	61.93

The results of energy and exergy efficiencies of all scenarios for the overall and cement process were given in Table 12.

Table 12. Overall and cement process efficiencies for all scenarios

	Overall		**Cement**	
	Energy efficiency	**Exergy efficiency**	**Energy efficiency**	**Exergy efficiency**
Base Scenario	61.60	20.21	61.60	20.21
Scenario 1	35.71	15.91	61.60	22.91
Scenario 2	42.27	15.27	61.60	21.90

The energy efficiency of the cement process for all scenarios was 61.60%. The reason was the energy requirement of the cement remained same for all scenarios. Only the source of energy has been changed, and this situation was expected to lead to various effects. For instance, in scenario 1 the heat requirement was sustained by coal and grid electricity was used. However, in scenario 1 the amount of coal used decreased. The

electricity supplied from the grid was replaced by the electricity produced by gas turbine. Instead of using coal, cement feedstocks were preheated, and hot pyrolysis gas products were combusted to produce heat. By this way some portion of the coal was eliminated. This leads to a decrease in specific energy consumption (SEC) and a decrease in CO_2 emissions. In scenario 2 the same situation was valid. The electricity was supplied by the grid. However, the heat requirement was sustained by combustion of hydrogen gas. The hydrogen gas produced was directly fed to the cement process to be combusted in rotary kiln. In this way all the coal was replaced by hydrogen gas. That leads to the removal of the CO_2 emissions caused by coal combustion.

When considering the overall energy efficiencies, the situation changes. Base scenario was the most efficient scenario among all of them with 61.60%. Scenario 1 has the lowest energy efficiency with 35.71%. The reason is a lot of units was used is scenario 1 and all of them requires energy. Besides, the amount of waste blade material fed to the pyrolysis reactor is so high. So, processing them requires so much energy. For scenario 2, energy efficiency was found as 42.27%. The responsible for the decrease of the efficiency for scenario 2 is the electrolyzer. It consumes a lot of electricity, and it is more than its energy production amount.

The energy efficiency of the PEM electrolyzer was found to be 56.5% in the study of Ahmadi, Dincer, and Rosen (2013). In the study of Musharavati, Ahmadi, and Khanmohammadi (2021) geothermal energy powered PEM electrolyzer was studied and energy and exergy efficiencies were obtained as 41% and 50% respectively Mohebali Nejadian, Ahmadi, and Houshfar (2023) examined three electrolyzer types that are SOEC, PEM and alkaline electrolyzer and their energy efficiencies were found as 13.15%, 13.04% and 12.41% respectively.

The overall exergy efficiency of base scenario was 20.21%. For scenario 1 and 2. they were 15.91% and 15.27% respectively. They were consistent with energy efficiency results because both of them decreased. From these results, it could be resulted that the system's potential to do work has decreased in scenario 1 and 2.

In the study of Madlool et al. (2012), it was presented that the exergy efficiency values range from 18% to 49%. Exergy efficiency results of this study were compatible with literature as it can be seen in Table 12. Atmaca and Yumrutaş (2014) found the overall energy efficiency as 59.37% and overall exergy efficiency as 38.99% In the study of

Ozturk and Yakut (2017), the energy and exergy efficiencies were calculated as 60.75% and 46.11 % respectively. In the study of Madlool et al. (2012) the energy and exergy efficiencies of cement production plant were found as 51% and 28% respectively, for the overall system.

Nevertheless, these systems must be considered for their SEC and CO_2 emission values. For each scenario SEC values was presented in Table 13 according to produced cement amounts which was 20.786 kg/s.

Table 13. Specific energy consumption (SEC) values for all scenarios

Scenarios	**Energy consumptions multiplied with primary energy factor (kW)**	**SEC (kJ/kg)**
Base Scenario	Combustion of coal: 62,200*1.1 Electricity for cement: 18,782*4.05	6951
Scenario 1 (without preheating)	Combustion of coal: 62,200*1.1 Pyrolysis heat requirement (natural gas): 6143*1.1	3617
Scenario 1	Combustion of coal: 29,313*1.1 Pyrolysis heat requirement (natural gas): 2886*1.1	1704
Scenario 2	Electricity for cement: 18,782*4.05 Electricity for electrolyzer: 99,228*4.05	22993

The term primary energy factor was used for a comprehensive assessment of energy consumption. It defines the ratio between the primary energy consumed and the final energy supplied. Coal and natural gas are considered primary energy because they are in natural form. So, the primary energy factor for coal and natural gas is 1.1. However, electricity is not primary energy. It has to follow a path to reach the consumer and losses energy. Primary energy factor for electricity is 4.05 (Osma-Pinto et al. 2015).

In base scenario, SEC was found as 6951 kJ/kg. Energy consumption was due to coal and electricity for the base scenario. SEC value decreased to 1704 kJ/kg for scenario 1. In here combusted coal amount was reduced and electricity was supplied with the

system's produced electricity. Besides, a heat requirement for pyrolysis exists. For the Brayton cycle units, there was no need for external energy sources. Moreover, there was net electricity produced in this scenario. In scenario 2, SEC was 22993 kJ/kg which was the highest. The reason is the energy requirement of electrolyzer.

Up to this point, the scenarios have more significant outcomes. From now on, CO_2 emissions data will be needed to have a more consistent opinion about scenarios. In Table 14 kg CO_2 emissions per kg cement produced were shown and calculated according to amount of cement produced (74,830 kg/h).

Table 14. CO_2 emissions for all scenarios

Scenarios	**CO_2 Emission Sources (kg/h)**	**CO_2 Emissions (kg CO_2/kg cement)**
Base Scenario	Combustion of coal: 17,706 Cement production: 16,417	0.456
Scenario 1 (without preheating)	Combustion of coal: 17,706 Cement production: 16,417 Pyrolysis gas: 1081 Combustion products: 5888	0.549
Scenario 1	Combustion of coal: 8322 Cement production: 16,417 Pyrolysis gas: 1081 Combustion of pyrolysis gas: 1266 Combustion products: 5888	0.441
Scenario 2	Cement production: 16,417	0.219

In base scenario CO2 emission was the highest as expected. It was 0.456 kg CO_2/kg cement and consistent with literature which was stated as 0.5 to 0.9 kg CO_2/kg cement (Fayomi et al. 2019). In here CO_2 emission sources were coal combustion and other emissions occurred during the production of cement. In scenario 1, emission was decreased to 0.441 kg CO_2/kg cement and its reason is the reduced coal amount. For scenario 2 emission data was the lowest with 0.219. In here there was only an emission that emerged while producing the cement. There was no coal combustion, so the emission values resulted as the minimum.

4.4. Sankey Diagrams

Sankey diagrams were used to visually represent energy and exergy flows. Sankey diagram shows the magnitudes and directions of energy/exergy flows in a system, allowing for better analysis of energy losses/exergy destructions and efficiency. It was used to facilitate the understanding of these systems and help to make more accurate analyses for energy and exergy flows.

For base scenario energy and exergy flow diagrams were presented in Figure 15.

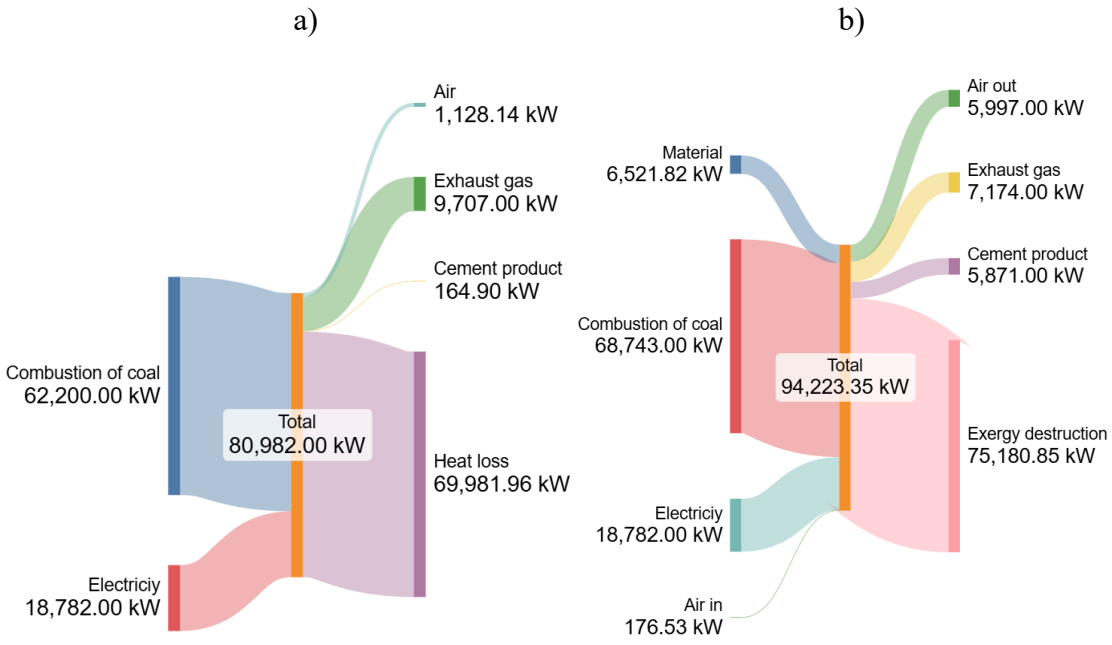

Figure 15. Sankey diagrams of base scenario a) energy flow b) exergy flow.

For base scenario heat loss in high amounts was observed in cement process. Consistent with this, a high amount of exergy destruction was observed. The reason is the dust and ash that comes from the cement process (Atmaca 2014). In addition, an insulation system was needed for this cement facility.

In Figure 16. Sankey energy and exergy diagrams for pyrolysis process were shown for scenario 1.

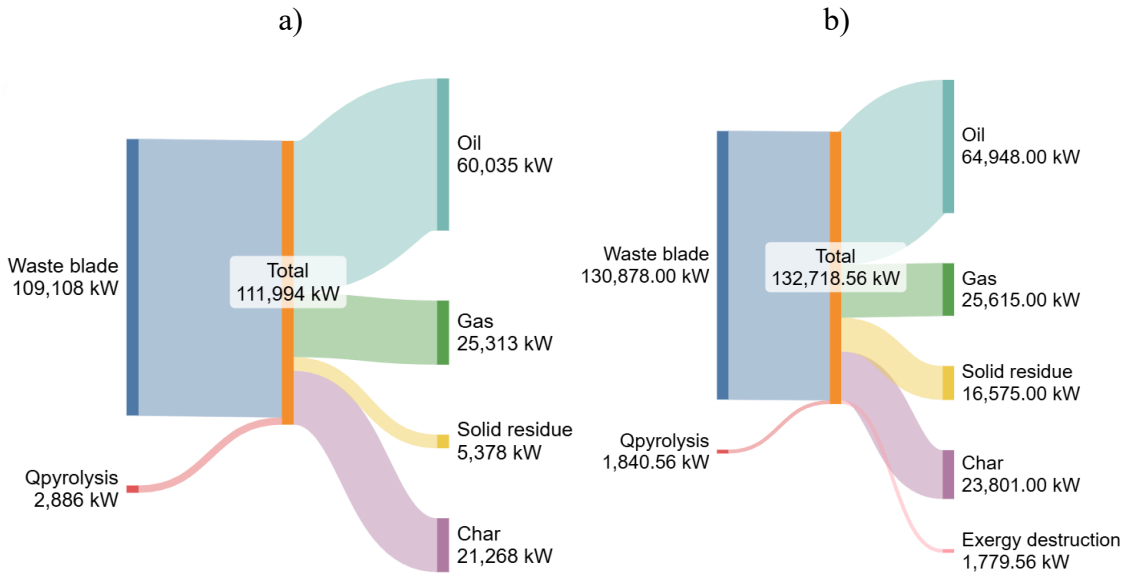

Figure 16. Sankey diagrams of scenario 1 for pyrolysis a) energy flow b) exergy flow.

The energy and exergy inlet flow of waste blade materials were in high amounts. It is because a high low rate of waste material was needed for the pyrolysis process to produce significant amounts of energy.

Sankey diagrams for Brayton cycle were represented in Figure 17.

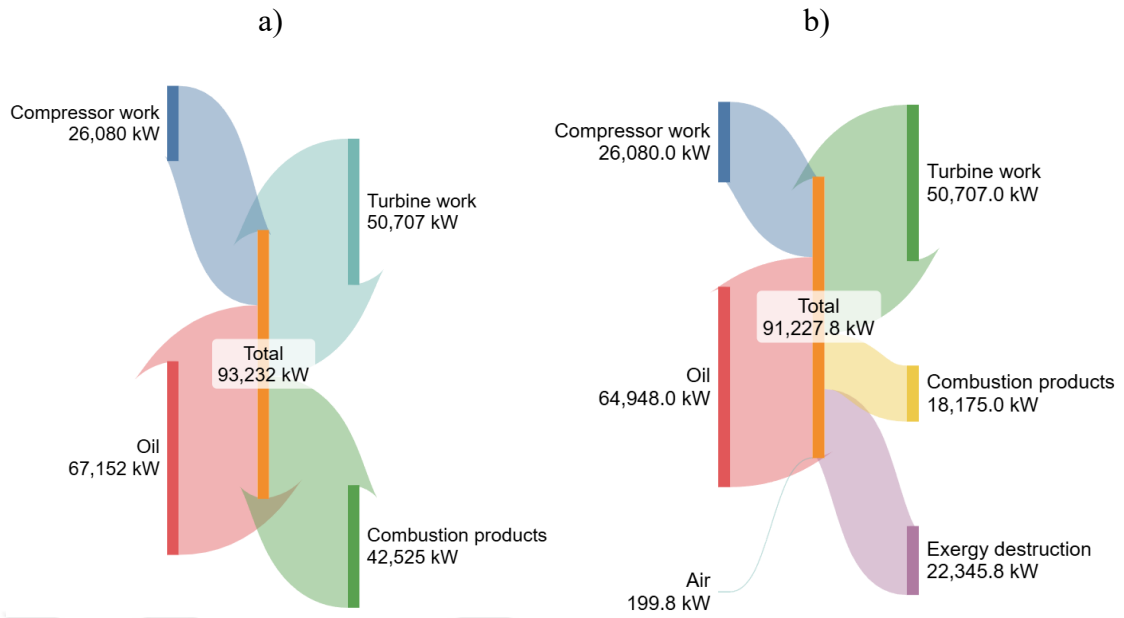

Figure 17. Sankey diagrams of scenario 1 for Brayton cycle a) energy flow b) exergy flow.

From Sankey diagram of Brayton cycle, it was understood that pyrolysis oil fed to gas turbine produces large amounts of turbine work and also potential energy carrier combustion products were produced.

Sankey diagrams of cement process for scenario 1 were shown in Figure 18.

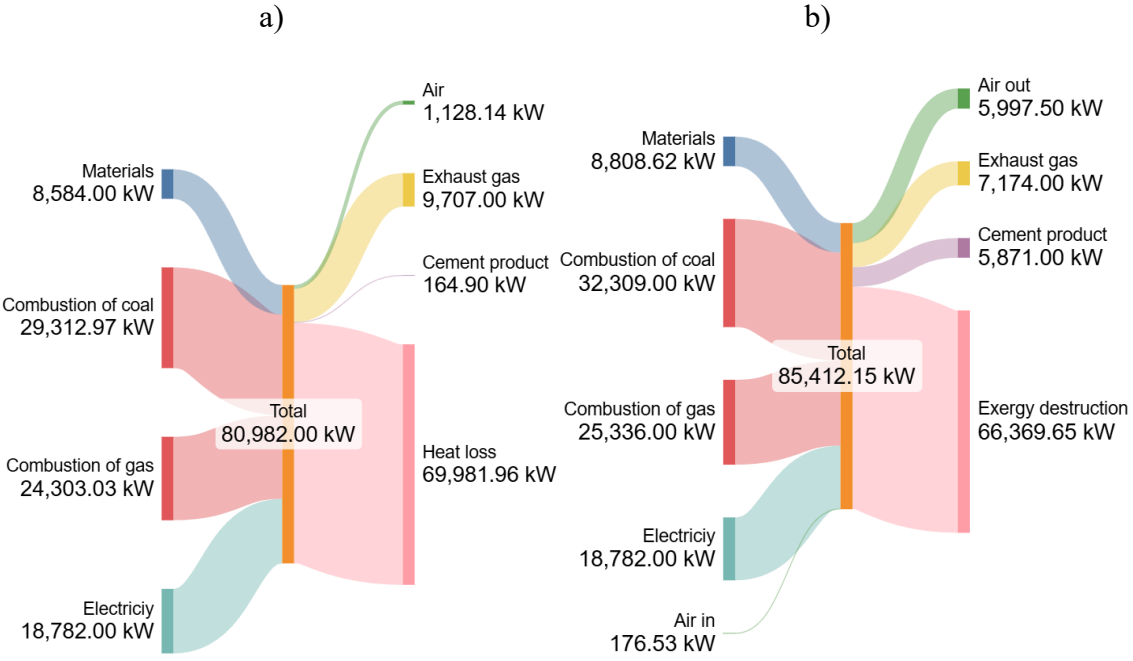

Figure 18. Sankey diagrams of scenario 1 for cement process a) energy flow b) exergy flow.

Sankey diagrams of cement process of scenario 1 shows similar results with base scenario. Since the amount of energy required was not altered so heat loss and exergy destructions are in large quantities.

In Figure 19, Sankey diagrams of cement process for scenario 2 were represented.

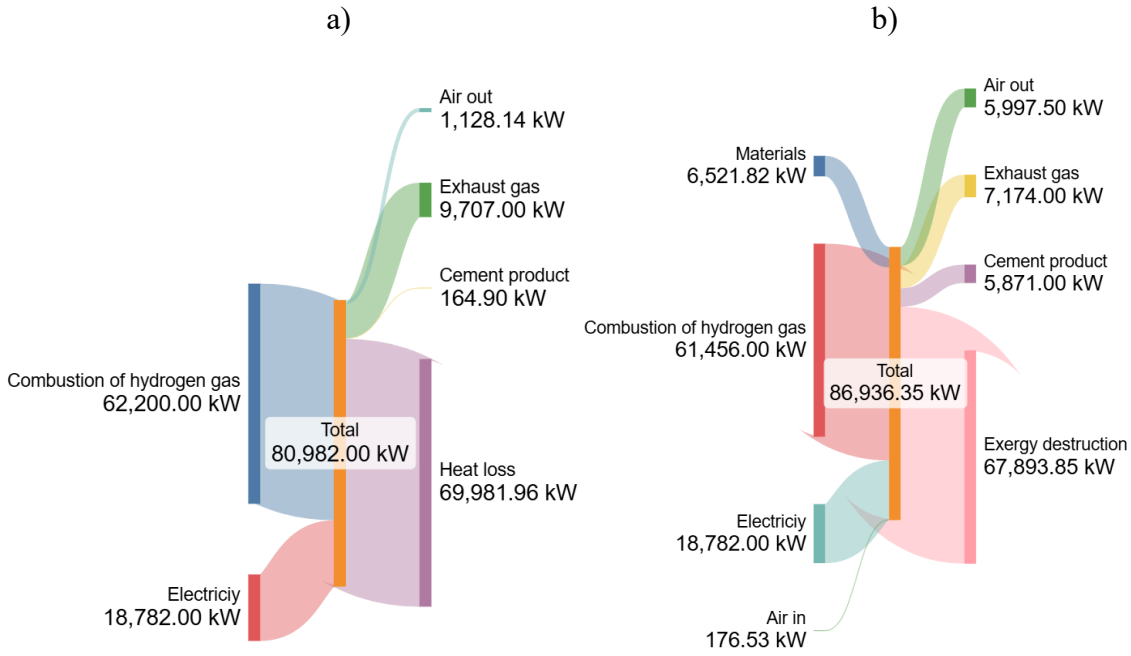

Figure 19. Sankey diagrams of scenario 2 for cement process a) energy flow b) exergy flow.

The same condition was valid for scenario 2 with scenario 1. Only the source of energy differs, and it could be evaluated by SEC and CO_2 emission data more precisely.

CHAPTER 5

CONCLUSION

Conventional cement production requires high energy input to process. It could be integrated into various systems to improve its efficiency with greener alternatives. Two different scenarios were investigated with the base scenario which was traditional cement production. The calculations of these systems were made with EES Software, and then the results were tabulated. According to the results, the energy efficiencies for cement were the same for all scenarios with 61.60%. The reason is, source of the energy was changed for each scenario, however the energy amount supplied to the cement process was the same.

The base scenario uses electrical power and coal. The first scenario includes the pyrolysis process and gas turbine to the cement production. Energy efficiency of cement process for scenario 1 was the lowest which was 35.71%. It could be the various units used in this scenario. The electricity was supplied from the electricity produced via gas turbine which was 50,707 kW. Besides, the solid residues of pyrolyzed wind turbine blade wastes were supplied to the cement process. For the first scenario there were hot streams which were potential energy carriers. These were combustion products (787 K), pyrolysis gas (823 K) and hot gas exhausts (562 K) from cement process. A preheating system was decided to be implied to the first scenario. Hot streams were fed to 4 different preheaters, and their energy potential was harnessed. They were used to heat feedstocks and replaced by some portion of coal. By this way, system becomes more externally independent. According to SEC and CO_2 emission results, both showed a decline. SEC and CO_2 emissions for base scenario were 6951 kJ/kg and 0.456 kg CO_2/kg cement respectively. For scenario 1, SEC and CO_2 emissions were 1704 kJ/kg and 0.441 kg CO_2/kg cement respectively. So, the preheating system had resulted successful.

The second scenario consists of a PEM electrolyzer included in the cement process. In addition to the base scenario, the coal was completely removed and replaced with hydrogen energy to supply heat to the cement facility. In here, the electricity was supplied from grid as the base scenario. In addition, 99,228 kW of electrical power for

PEM electrolyzer was needed. This energy requirement was affected the overall efficiencies, which was decreased to 42.27% (energy efficiency) and 15.27% (exergy efficiency) according to base scenario. Besides, SEC was the highest for scenario 2 which was 22993 kJ/kg. However, the minimum CO_2 emissions were observed with this scenario which was 1704 kg CO_2/kg cement.

The overall exergy efficiency of base scenario, scenario 1 and scenario 2 were 20.21%, 15.91% and 15.27% respectively. According to that, system's potential to do work has decreased in scenario 1 and 2.

This study was conducted in terms of exploring alternative green production methods for cement process. Considering all of these, the following conclusion can be obtained: Scenario 1 did not have the highest efficiency results. However, its SEC was the lowest and CO_2 emission was lower than the conventional production method. Under these circumstances it could be convenient because it is greener and consumes less energy than base scenario. So, this was the aim at the beginning of this study. However, its applicability to the real world would be considered. An economic analysis could be performed and various improvements might be applied.

REFERENCES

Abutorabi, Hossein, and Ehsan Kianpour. 2022. “Modeling, Exergy Analysis and Optimization of Cement Plant Industry.” *Journal of Mechanical and Energy Engineering* 6 (1): 55–66. https://doi.org/10.30464/jmee.2022.6.1.55.

“ACTIVITY REPORT 2 0 2 3.” n.d. www.cembureau.eu.

Ahmadi, Pouria, Ibrahim Dincer, and Marc A. Rosen. 2013a. “Energy and Exergy Analyses of Hydrogen Production via Solar-Boosted Ocean Thermal Energy Conversion and PEM Electrolysis.” *International Journal of Hydrogen Energy* 38 (4): 1795–1805. https://doi.org/10.1016/j.ijhydene.2012.11.025.

———. 2013b. “Energy and Exergy Analyses of Hydrogen Production via Solar-Boosted Ocean Thermal Energy Conversion and PEM Electrolysis.” *International Journal of Hydrogen Energy* 38 (4): 1795–1805. https://doi.org/10.1016/j.ijhydene.2012.11.025.

Atienza-Martínez, María, Javier Ábrego, José Francisco Mastral, Jesús Ceamanos, and Gloria Gea. 2018. “Energy and Exergy Analyses of Sewage Sludge Thermochemical Treatment.” *Energy* 144 (February):723–35. https://doi.org/10.1016/j.energy.2017.12.007.

Atmaca, Adem. 2014a. “GRADUATE SCHOOL OF NATURAL & APPLIED SCIENCES INCREASING EFFICIENCY AND REDUCING POLLUTANTS IN CEMENT INDUSTRY BY THERMODYNAMIC AND EXERGOECONOMIC METHODS Ph.D THESIS IN MECHANICAL ENGINEERING.”

———. 2014b. “GRADUATE SCHOOL OF NATURAL & APPLIED SCIENCES INCREASING EFFICIENCY AND REDUCING POLLUTANTS IN CEMENT INDUSTRY BY THERMODYNAMIC AND EXERGOECONOMIC METHODS Ph.D THESIS IN MECHANICAL ENGINEERING.”

Atmaca, Adem, Mehmet Kanoglu, and Mohamed Gadalla. 2012. “Thermodynamic Analysis of a Pyroprocessing Unit of a Cement Plant: A Case Study Thermodynamic Analysis of a Pyroprocessing Unit of a Cement Plant.” *Int. J. Exergy*. Vol. 11.

Atmaca, Adem, and Recep Yumrutaş. 2014a. “Thermodynamic and Exergoeconomic Analysis of a Cement Plant: Part II - Application.” *Energy Conversion and Management* 79:799–808. https://doi.org/10.1016/j.enconman.2013.11.054.

———. 2014b. “Thermodynamic and Exergoeconomic Analysis of a Cement Plant: Part II - Application.” *Energy Conversion and Management* 79:799–808. https://doi.org/10.1016/j.enconman.2013.11.054.

Benjatikul, Kitkanya, Hansa Mahamongkol, and Paveena Wongtrakul. 2020. “Sunscreen Properties of Marl.” *Journal of Oleo Science* 69 (1): 73–82. https://doi.org/10.5650/jos.ess19232.

“BIOMASS AS A SUSTAINABLE ENERGY SOURCE FOR THE FUTURE.” n.d.

Caglar, Basar, Duygu Tavsanci, and Emrah Biyik. 2021. “Multiparameter-Based Product, Energy and Exergy Optimizations for Biomass Gasification.” *Fuel* 303 (November). https://doi.org/10.1016/j.fuel.2021.121208.

Cheng, Guangwen, Song Yang, Xiaoqian Wang, Zhongxu Guo, and Ming Cai. 2023. “Study on the Recycling of Waste Wind Turbine Blades.” *Journal of Engineering Research (Kuwait)* 11 (3): 13–17. https://doi.org/10.1016/J.JER.2023.100070.

Cruz, Jose Nolasco, Irma Pérez Hernández, María de Lourdes Castellanos Villalobo, Angélica Pérez Henández, and Juan José López Ávila. 2023. “Thermochemical Degradation of Polypropylene: Energy and Exergy Analysis in a Tubular Reactor.” *Journal of Ecological Engineering* 24 (5): 14–21. https://doi.org/10.12911/22998993/161079.

Ebrahimi, Amirreza, and Ehsan Houshfar. 2022. “Thermodynamic Analysis and Optimization of the Integrated System of Pyrolysis and Anaerobic Digestion.” *Process Safety and Environmental Protection* 164 (August):582–94. https://doi.org/10.1016/j.psep.2022.06.043.

“Energy and Exergy Assessment and Heat Recovery on Rotary Kiln of Cement Plant for Cooling Effect Production by Using Vapor Absorption Refrigeration System.” 2020. *Iranian Journal of Energy and Environment* 11 (2). https://doi.org/10.5829/ijee.2020.11.02.03.

Fakehi, Amir Hossein, Somayeh Ahmadi, and Mohammad Rezaie Mirghaed. 2015. "Optimization of Operating Parameters in a Hybrid Wind-Hydrogen System Using Energy and Exergy Analysis: Modeling and Case Study." *Energy Conversion and Management* 106 (December):1318–26. https://doi.org/10.1016/j.enconman.2015.10.003.

Falcão, D. S., and A. M.F.R. Pinto. 2020. "A Review on PEM Electrolyzer Modelling: Guidelines for Beginners." *Journal of Cleaner Production*. Elsevier Ltd. https://doi.org/10.1016/j.jclepro.2020.121184.

Fayomi, G. U., S. E. Mini, O. S.I. Fayomi, and A. A. Ayoola. 2019. "Perspectives on Environmental CO2 Emission and Energy Factor in Cement Industry." In *IOP Conference Series: Earth and Environmental Science*. Vol. 331. Institute of Physics Publishing. https://doi.org/10.1088/1755-1315/331/1/012035.

Ghalandari, Vahab. 2022. "A Comprehensive Study on Energy and Exergy Analyses for an Industrial-Scale Pyro-Processing System in Cement Plant." *Cleaner Energy Systems* 3 (December). https://doi.org/10.1016/j.cles.2022.100030.

Guo, Huan, Yi Zhang, Yujie Xu, Xuezhi Zhou, and Haisheng Chen. 2024. "Derived Energy Storage Systems from Brayton Cycle." *IScience* 27 (4). https://doi.org/10.1016/j.isci.2024.109460.

Hajimohammadi Tabriz, Zahra, Muhammad Hadi Taheri, Leyla Khani, Başar Çağlar, and Mousa Mohammadpourfard. 2024. "Enhancing a Bio-Waste Driven Polygeneration System through Artificial Neural Networks and Multi-Objective Genetic Algorithm: Assessment and Optimization." *International Journal of Hydrogen Energy* 58 (March):1486–1503. https://doi.org/10.1016/j.ijhydene.2024.01.350.

"High-Emitting Sectors: Challenges and Opportunities for Low-Carbon Suppliers." 2024a. www.deloitte.com/about.

"High-Emitting Sectors: Challenges and Opportunities for Low-Carbon Suppliers." ——. 2024b. www.deloitte.com/about.

Hopper. n.d. "Glass Fibers."

Ismail, Mohamed M., and Ibrahim Dincer. 2023. "Development and Evaluation of an Integrated Waste to Energy System Based on Polyethylene Plastic Wastes Pyrolysis

for Production of Hydrogen Fuel and Other Useful Commodities." *Fuel* 334 (February). https://doi.org/10.1016/j.fuel.2022.126409.

Jalili, M, R Cheraghi, M M Reisi, and R Ghasempour. 2020. "Energy and Exergy Assessment of a New Heat Recovery Method in a Cement Factory" 1 (1): 123–34. https://doi.org/10.22044/rera.2020.9123.1017.

Jani, Hardik K., Surendra Singh Kachhwaha, Garlapati Nagababu, and Alok Das. 2022. "A Brief Review on Recycling and Reuse of Wind Turbine Blade Materials." *Materials Today: Proceedings* 62 (P13): 7124–30. https://doi.org/10.1016/j.matpr.2022.02.049.

Jery, Atef El, Hayder Mahmood Salman, Rusul Mohammed Al-Khafaji, Maadh Fawzi Nassar, and Mika Sillanpää. 2023. "Thermodynamics Investigation and Artificial Neural Network Prediction of Energy, Exergy, and Hydrogen Production from a Solar Thermochemical Plant Using a Polymer Membrane Electrolyzer." *Molecules* 28 (6). https://doi.org/10.3390/molecules28062649.

John, John P. 2020. "Parametric Studies of Cement Production Processes." *Journal of Energy* 2020 (February):1–17. https://doi.org/10.1155/2020/4289043.

Kalkanis, K., C. S. Psomopoulos, S. Kaminaris, G. Ioannidis, and P. Pachos. 2019. "Wind Turbine Blade Composite Materials - End of Life Treatment Methods." In *Energy Procedia*, 157:1136–43. Elsevier Ltd. https://doi.org/10.1016/j.egypro.2018.11.281.

Koroneos, C, G Roumbas, and N Moussiopoulos. 2005. "Exergy Analysis of Cement Production." *Int. J. Exergy*. Vol. 2. www.titan.gr.

Kotas, T. J.. 1985. *The Exergy Method of Thermal Plant Analysis*. Butterworths.

Li, Ruochen, Gongxiang Song, Dexin Huang, Song Hu, Francesco Fantozzi, Ahmed Hassan, Pietro Bartocci, et al. 2024. "Comparative Study of Process Simulation, Energy and Exergy Analyses of Solar Enhanced Char-Cycling Biomass Pyrolysis Process." *Energy Conversion and Management* 302 (February). https://doi.org/10.1016/j.enconman.2024.118082.

Liu, P., and C. Y. Barlow. 2016. "The Environmental Impact of Wind Turbine Blades." In *IOP Conference Series: Materials Science and Engineering*. Vol. 139. Institute of Physics Publishing. https://doi.org/10.1088/1757-899X/139/1/012032.

Liu, Pu, and Claire Y. Barlow. 2017. “Wind Turbine Blade Waste in 2050.” *Waste Management* 62 (April):229–40. https://doi.org/10.1016/j.wasman.2017.02.007.

Liu, Rongtang, Ming Liu, Peipei Fan, Yongliang Zhao, and Junjie Yan. 2018. “Thermodynamic Study on a Novel Lignite Poly-Generation System of Electricity-Gas-Tar Integrated with Pre-Drying and Pyrolysis.” *Energy* 165 (December):140–52. https://doi.org/10.1016/j.energy.2018.09.169.

Ma, Songsong, Linjun Li, Ryuta Kohama, Hironori Nakajima, and Kohei Ito. n.d. “Effects of Temperature and Pressure on the Limiting Current Density of PEM Electrolysis Cells Based on a Theoretical Prediction Model and Experiments.” https://ssrn.com/abstract=4717500.

Madlool, N. A., R. Saidur, N. A. Rahim, M. R. Islam, and M. S. Hossian. 2012a. “An Exergy Analysis for Cement Industries: An Overview.” *Renewable and Sustainable Energy Reviews*. https://doi.org/10.1016/j.rser.2011.09.013.

———. 2012b. “An Exergy Analysis for Cement Industries: An Overview.” *Renewable and Sustainable Energy Reviews*. https://doi.org/10.1016/j.rser.2011.09.013.

Marmier, A. 2000. “Decarbonisation Options for the Cement Industry.” In . https://doi.org/10.2760/174037.

Millet, Pierre, and Sergey A. Grigoriev. 2014. “Electrochemical Characterization and Optimization of a PEM Water Electrolysis Stack for Hydrogen Generation.” *Chemical Engineering Transactions* 41 (Special Issue): 7–12. https://doi.org/10.3303/CET1441002.

Mohebali Nejadian, Mehrnaz, Pouria Ahmadi, and Ehsan Houshfar. 2023a. “Comparative Optimization Study of Three Novel Integrated Hydrogen Production Systems with SOEC, PEM, and Alkaline Electrolyzer.” *Fuel* 336 (March). https://doi.org/10.1016/j.fuel.2022.126835.

———. 2023b. “Comparative Optimization Study of Three Novel Integrated Hydrogen Production Systems with SOEC, PEM, and Alkaline Electrolyzer.” *Fuel* 336 (March). https://doi.org/10.1016/j.fuel.2022.126835.

Moradi Nafchi, Faeze, Ebrahim Afshari, Ehsan Baniasadi, and Nader Javani. 2019. “A Parametric Study of Polymer Membrane Electrolyser Performance, Energy and

Exergy Analyses." *International Journal of Hydrogen Energy* 44 (34): 18662–70. https://doi.org/10.1016/j.ijhydene.2018.11.081.

Musharavati, Farayi, Pouria Ahmadi, and Shoaib Khanmohammadi. 2021a. "Exergoeconomic Assessment and Multiobjective Optimization of a Geothermal-Based Trigeneration System for Electricity, Cooling, and Clean Hydrogen Production." *Journal of Thermal Analysis and Calorimetry* 145 (3): 1673–89. https://doi.org/10.1007/s10973-021-10793-4.

———. 2021b. "Exergoeconomic Assessment and Multiobjective Optimization of a Geothermal-Based Trigeneration System for Electricity, Cooling, and Clean Hydrogen Production." *Journal of Thermal Analysis and Calorimetry* 145 (3): 1673–89. https://doi.org/10.1007/s10973-021-10793-4.

Nami, Hossein, and Amjad Anvari-Moghaddam. 2020. "Small-Scale CCHP Systems for Waste Heat Recovery from Cement Plants: Thermodynamic, Sustainability and Economic Implications." *Energy* 192 (February). https://doi.org/10.1016/j.energy.2019.116634.

Ni, Meng, Michael K.H. Leung, and Dennis Y.C. Leung. 2008. "Energy and Exergy Analysis of Hydrogen Production by a Proton Exchange Membrane (PEM) Electrolyzer Plant." *Energy Conversion and Management* 49 (10): 2748–56. https://doi.org/10.1016/j.enconman.2008.03.018.

Osma-Pinto, Germán Alfonso, David Andrés Sarmiento-Nova, Nelly Catherine Barbosa-Calderón, and Gabriel Ordóñez-Plata. 2015. "Energy Considerations of Social Dwellings in Colombia According to the NZEB Concept." *DYNA (Colombia)* 82 (192): 120–30. https://doi.org/10.15446/dyna.v82n192.48587.

Ozturk, M, and A K Yakut. 2017. "Energetic and Exergetic Performance Investigation of a Cement Facility for Clinker Production." *Int. J. Exergy*. Vol. 23.

Parvez, Ashak Mahmud, Tao Wu, Muhammad T. Afzal, Sannia Mareta, Tianbiao He, and Ming Zhai. 2019. "Conventional and Microwave-Assisted Pyrolysis of Gumwood: A Comparison Study Using Thermodynamic Evaluation and Hydrogen Production." *Fuel Processing Technology* 184 (February):1–11. https://doi.org/10.1016/j.fuproc.2018.11.007.

Peters, Jens F., Fontina Petrakopoulou, and Javier Dufour. 2014. “Exergetic Analysis of a Fast Pyrolysis Process for Bio-Oil Production.” *Fuel Processing Technology* 119:245–55. https://doi.org/10.1016/j.fuproc.2013.11.007.

Rao, R. Bhima, L. Besra, B. R. Reddy, and G. N. Banerjee. 1997. “Effect of Pretreatment on Magnetic Separation of Ferruginous Minerals in Bauxite.” *Magnetic and Electrical Separation* 8 (2): 115–23. https://doi.org/10.1155/1997/53574.

Singh, Rohitashva K, and Surendra P Shah. n.d. “CARBON CAPTURE AND UTILIZATION FOR READY MIX CONCRETE.”

Sivaraman, Subramaniyasharma, Saravanan Ramiah Shanmugam, Bhuvaneshwari Veerapandian, and Ponnusami Venkatachalam. 2023. “Understanding the Pyrolysis Kinetics, Thermodynamic, and Environmental Sustainability Parameters of Sesamum Indicum Crop Residue.” *Environmental Research Communications* 5 (12). https://doi.org/10.1088/2515-7620/ad16f2.

Šveda, Mikuláš, and Radomír Sokolář. 2013. “The Effect of Firing Temperature on the Irreversible Expansion, Water Absorption and Pore Structure of a Brick Body during Freeze-Thaw Cycles.” *Medziagotyra* 19 (4): 465–70. https://doi.org/10.5755/j01.ms.19.4.2741.

“Technology Roadmap Low-Carbon Transition in the Cement.” n.d. www.wbcsdcement.org.

Temireyeva, Aknur, Yerbol Sarbassov, and Dhawal Shah. 2024. “Process Simulation of Flax Straw Pyrolysis with Kinetic Reaction Model: Experimental Validation and Exergy Analysis.” *Fuel* 367 (July). https://doi.org/10.1016/j.fuel.2024.131494.

“Thermal Design and Optimization (Textbook).” n.d.

Wang, Xinyu, Wei Lv, Li Guo, Ming Zhai, Peng Dong, and Guoli Qi. 2016. “Energy and Exergy Analysis of Rice Husk High-Temperature Pyrolysis.” *International Journal of Hydrogen Energy* 41 (46): 21121–30. https://doi.org/10.1016/j.ijhydene.2016.09.155.

Worrell, E. 2014. “Cement and Energy.” In *Reference Module in Earth Systems and Environmental Sciences*. Elsevier. https://doi.org/10.1016/b978-0-12-409548-9.09057-6.

Xu, Ming xin, Hai wen Ji, Xiang xi Meng, Jie Yang, Ya chang Wu, Jin yi Di, Hao Jiang, and Qiang Lu. 2023. “Effects of Core Materials on the Evolution of Products during the Pyrolysis of End-of-Life Wind Turbine Blades.” *Journal of Analytical and Applied Pyrolysis* 175 (October). https://doi.org/10.1016/j.jaap.2023.106222.

Xu, Ming xin, Hai wen Ji, Ya chang Wu, Jin yi Di, Xiang xi Meng, Hao Jiang, and Qiang Lu. 2023. “The Pyrolysis of End-of-Life Wind Turbine Blades under Different Atmospheres and Their Effects on the Recovered Glass Fibers.” *Composites Part B: Engineering* 251 (February). https://doi.org/10.1016/j.compositesb.2022.110493.

Yang, Wooyoung, Ki Hyun Kim, and Jechan Lee. 2022. “Upcycling of Decommissioned Wind Turbine Blades through Pyrolysis.” *Journal of Cleaner Production*. Elsevier Ltd. https://doi.org/10.1016/j.jclepro.2022.134292.

Zhang, Yutao, Guozhao Ji, Dexiao Ma, Chuanshuai Chen, Yinxiang Wang, Weijian Wang, and Aimin Li. 2020. “Exergy and Energy Analysis of Pyrolysis of Plastic Wastes in Rotary Kiln with Heat Carrier.” *Process Safety and Environmental Protection* 142 (October):203–11. https://doi.org/10.1016/j.psep.2020.06.021.

APPENDIX A.

Thermodynamic Properties in Tabulated Form

Table 15. Thermodynamic properties, energy and exergy rates in the plant with respect to state points

State no.	Fluid/power	Mass flow rate (kg/s)	Temperature (K)	Energy rate (kW)	Exergy rate (kW)
1	Coarse limestone	20.62	305	84.56	0.69
2	Crusher electrical power	–	–	459.18	459.18
3	Fine limestone	20.62	322	372.08	13.011
4	Crusher boundary heat loss	–	–	171.66	171.66
5	Marl	12.01	295	38.41	0.33
6	Clay	4.13	295	18.98	0.16
7	Iron ore	0.37	295	1.16	0.01
8	Bauxite	0.37	295	1.2	0.01
9	Moisture	4.17	295	87.25	0.74
10	Raw mill electrical power	–	–	3250	3250
11	Hot gas from tower	18.43	567	7402.19	2206.26
12	Air leakages	1.127	295	5.69	0.05
13	Hot gas exhaust	18.429	380	2405.04	310.41
14	Raw mill boundary heat loss	–	–	4438.79	4438.79
15	Raw mix (farine)	45.618	380	3777.13	487.49
16	Pyroprocessing tower electrical power	–	–	5000	5000
17	Hot gas from rotary kiln	18.429	1725	40836.29	25798.22
18	Air leakages	7.007	300	0	0
19	Hot farine	28.74	1011	20638.8	10058.91
20	Pyroprocessing tower boundary heat loss	–	–	22790.31	22790.31
21	Exhaust	18.429	227	4191.96	1057.58
22	Rotary kiln electrical power	–	–	4341.5	4341.5
23	Secondary air from cooler	24.864	1083.913	23240.13	12047.6
24	Coal	2	344	112.6	9.34
25	Primary air	2.741	290	87.48	4.23
26	Air leakages	3.579	710	1581	603.56
27	Rotary kiln boundary heat loss	–	–	12542.5	12542.51
28	Hot clinker	18.111	1550	24293.94	14921.93
29	Coarse coal	2	305	11	0.09
30	Coal mill electrical power	–	–	1504	1504
31	Hot gas from cooler	4.97	707	2428.73	894.07
32	Coal mill boundary heat loss	–	–	2670.36	2670.36
33	Fresh air	47	313	607.03	12.78
34	Grate clinker cooler electrical power	–	–	1873	1873
35	Grate clinker cooler boundary heat loss	–	–	4510	4510
36	Cold clinker	18	390	1408.37	176.68
37	Gypsum	0.922	310	7.56	0.12
38	Limestone	0.986	310	7.29	0.12
39	Cement mill electrical power	–	–	2202	2202
40	Cement mill boundary heat loss	–	–	538.67	538.67
41	Air leakages	1.142	381	93.43	10.72
42	Cement	20.886	381	1725.6	198.02
43	Packaging unit electrical power	–	–	152	152
44	Packaging unit boundary heat loss	–	–	152.01	152.01
45	Air leakages	0.1	310	1.01	0.016
46	Finished cement	20.786	310	212.02	3.46

Table 16. EES result of base scenario

State name	State #	ṁ (kg/s)	T(K)	Energy rate (kW)	Exergy rate (kW)
Limestone	1	20.62	298.20	0.00	1041.00
Marl	2	12.01	298.20	0.00	761.20
Clay	3	4.13	298.20	0.00	1750.00
Iron ore	4	0.37	298.20	0.00	47.11
Bauxite	5	0.37	298.20	0.00	644.60
Moisture	6	4.17	298.20	0.00	2199.00
Gypsum	7	0.92	298.20	0.00	29.12
Limestone	8	0.99	298.20	0.00	49.79
Coal	9	2.00	298.20	62200.00	68743.00
Primary air	10	2.74	298.20	0.00	9.73
Fresh air	11	47.00	298.20	0.00	166.80
Exhaust	12	18.43	523.00	4222.00	1141.00
Hot gas exhaust	13	38.18	380.00	3263.00	4654.00
Air leakages	14	1.13	298.20	0.00	4.00
Air leakages	15	7.01	300.00	13.04	24.90
Air leakages	16	3.58	710.00	1006.00	5949.00
Air leakages	17	1.14	381.00	95.48	15.28
Air leakages	18	0.10	310.00	13.62	4.32
Hot gas exhaust	19	4.97	707.00	2222.00	1379.00
Finished cement	20	20.79	310.00	164.90	5871.00

Table 17. EES result of scenario 1

State name	State #	ṁ (kg/s)	T(K)	Energy rate (kW)	Exergy rate (kW)
Inorganic	1	11.89	298.20	0.00	14240.00
Organic	2	3.96	298.20	105851.00	115622.00
Inorganic	3	11.89	545.00	2384.00	14901.00
Organic	4	3.96	545.00	106144.00	115702.00
Inorganic	5	11.89	595.00	2904.00	15148.00
Organic	6	3.96	595.00	106204.00	115730.00
Gas	7	0.97	823.20	25313.00	25615.00
Oil	8	2.31	823.20	60035.00	64948.00
Solid residue	9	11.89	823.20	5378.00	16575.00
Char	10	0.69	823.20	21268.00	23801.00
Air	11	79.04	298.20	0.00	199.80
Air	12	79.04	614.40	26080.00	24306.00
Air	13	79.04	850.00	46604.00	36058.00
Combustion products	14	81.35	1520.00	113756.00	85553.00
Combustion products	15	81.35	1007.00	63049.00	32065.00
Combustion products	16	81.35	787.30	42525.00	18175.00
Combustion products	17	81.35	759.00	39943.00	16589.00
Combustion products	18	81.35	734.00	37677.00	15228.00
Gas	19	0.97	603.00	24831.00	25336.00
Limestone	20	20.62	298.20	0.00	1041.00
Marl	21	12.01	298.20	0.00	761.20
CaCO3	22	32.63	485.00	5849.00	2956.00
CaCO3	23	32.63	563.00	8584.00	4089.00
Clay	24	4.13	298.20	0.00	1750.00
Iron ore	25	0.37	298.20	0.00	47.11
Bauxite	26	0.37	298.20	0.00	644.60
Moisture	27	4.17	298.20	0.00	2199.00
Gypsum	28	0.92	298.20	0.00	29.12
Limestone	29	0.99	298.20	0.00	49.79
Coal	30	0.94	298.20	29234.00	32309.00
Primary air	31	2.74	298.20	0.00	9.73
Fresh air	32	47.00	298.20	0.00	166.80
Exhaust	33	18.43	523.00	4222.00	1141.00
Hot gas exhaust	34	38.18	380.00	3263.00	4654.00
Air leakages	35	1.13	298.20	0.00	4.00

(cont. on next page)

Table 17 (cont.)

Air leakages	36	7.01	300.00	13.04	24.90
Air leakages	37	3.58	710.00	1006.00	5949.00
Air leakages	38	1.14	381.00	95.48	15.28
Air leakages	39	0.10	310.00	13.62	4.32
Hot gas exhaust	40	4.97	707.00	2222.00	1379.00
Finished cement	41	20.79	310.00	164.90	5871.00
Exhaust mix	42	23.40	562.00	6311.00	1873.00
Exhaust mix	43	23.40	351.00	1246.00	182.00

Table 18. EES result of scenario 2

State name	State #	ṁ (kg/s)	T(K)	Energy rate (kW)	Exergy rate (kW)
Water	1	4.63	298.20	0.00	2443.00
Oxygen	2	4.11	343.00	169.70	522.00
Hydrogen	3	0.52	343.00	62530.00	61456.00
Limestone	4	20.62	298.20	0.00	1041.00
Marl	5	12.01	298.20	0.00	761.20
Clay	6	4.13	298.20	0.00	1750.00
Iron ore	7	0.37	298.20	0.00	47.11
Bauxite	8	0.37	298.20	0.00	644.60
Moisture	9	4.17	298.20	0.00	2199.00
Gypsum	10	0.92	298.20	0.00	29.12
Limestone	11	0.99	298.20	0.00	49.79
Primary air	12	2.74	298.20	0.00	9.73
Fresh air	13	47.00	298.20	0.00	166.80
Exhaust	14	18.43	523.00	4222.00	1141.00
Hot gas exhaust	15	38.18	380.00	3263.00	4654.00
Air leakages	16	1.13	298.20	0.00	4.00
Air leakages	17	7.01	300.00	13.04	24.90
Air leakages	18	3.58	710.00	1006.00	5949.00
Air leakages	19	1.14	381.00	95.48	15.28
Air leakages	20	0.10	310.00	13.62	4.32
Hot gas exhaust	21	4.97	707.00	2222.00	1379.00